eman ta zabal zazu

Universidad del País Vasco
Euskal Herriko Unibertsitatea

KIMIKA ZIENTZIEN FAKULTATEA

FACULTAD DE CIENCIAS QUÍMICAS

Universidad del País Vasco/Euskal Herriko Unibertsitatea

Facultad de Química/Kimika Fakultatea

Kimikako Gradua

FINAL DEGREE PROJECT

Polymers for the preparation of heterogeneous catalysts

Author: Mario Martinez Yubero

Director: Prof. Oihane Sanz Iturralde

Donostia/San Sebastian, June of 2021

INDEX

ABSTRACT

In this work it has been studied the effect different polymers (or also the same polymer with different properties) can make in the preparation of catalysts Ni-La/Al_2O_3 by the wet impregnation with excess of water. In order to do that, the catalysts were first prepared with the method "All in one", a method that was developed in our laboratory group. This method consists on the preparation of aqueous suspensions with every component to obtain the final catalyst: the support, the precursor salt of the active material and the additives, were polymers are introduced. The method allows us to create the catalysts in suspensions that can be used directly for the structured substrates coating, or after drying and calcinating this suspensions, slurried catalysts in powder form can be obtained to use them for each characterization technique.

After preparing the aqueous suspensions, they were characterised by viscosimetry in order to find out the changes on the viscosity made by the addition of the different polymers, and after drying and calcinating them, the obtained slurried catalysts were characterized by different techniques: N_2 physisorption, CO chemisorption, temperature programmed reduction and X-ray diffraction. This characterization was made to study the effect of the added polymer in the catalyst, which was supposed to improve the effect on the Sabatier's reaction. The results show that depending on the polymer added to the catalyst formulation, the utility of this would change, also that with the addition of the same polymer, modifying the molecular weight or the hydrolysis degree, the results obtained would be different, making some polymers more useful than others.

On the other hand, it had been previously discovered that the use of polyvynil alcohol (PVA) and Ni content influences directly in the properties of catalysts obtained by the "All in one" method. PVA allows to control nickels particle size managing to have a higher dispersion and, as a consequence, the number of active centres is larger. In this work, PVA, polyvynilpyrrolidone (PVP) and polyethylene glycol (PEG) will be used to improve the dispersion and as a consequence, improve the active centres.

RESUMEN

En este trabajo se ha estudiado el efecto que causan diferentes polímeros (o el mismo polímero con diferentes propiedades) en la preparación de catalizadores Ni-La/Al_2O_3 mediante la impregnación húmeda con exceso de agua. Con ese objetivo, los catalizadores fueron preparados usando el método "Todo en uno", un método desarrollado en nuestro grupo de laboratorio. Este método consiste en la preparación de una suspensión acuosa con todos los componentes para obtener un catalizador final: el soporte, la sal precursora del material activo y los aditivos, en los cuales se incluye el polímero. El método nos permite la creación de catalizadores en suspensión que pueden ser usados directamente para el recubrimiento de los sustratos estructurados, o tras el secado y calcinación de estas suspensiones, se pueden obtener catalizadores suspendidos en polvo para las técnicas de caracterización.

Las suspensiones acuosas fueron caracterizadas por medio de viscosimetrías para observar los cambios en la viscosidad con la adición de los diferentes polímeros, y una vez secadas y calcinadas, obteniendo así los catalizadores suspendidos, fueron caracterizados con diferentes técnicas: fisisorción N_2, quimisorción de CO, reducción programada de temperatura (TPR) y difracción de rayos X. Esta caracterización fue hecha para estudiar el efecto que causaba el polímero añadido en el catalizador, lo que debería de crear una mejora para las reacciones de Sabatier. Los resultados mostraron que, dependiendo del polímero usado en la formulación, la utilidad del catalizador variaba, también añadiendo el mismo polímero, con cambios en el peso molecular o en el grado de hidrólisis del mismo, se obtuvieron diversos resultados, siendo algunos polímeros más útiles que otros.

Por otro lado, fue descubierto previamente que el uso de poli vinil alcohol (PVA) y Ni influye directamente en las propiedades de los catalizadores obtenidos por el método "Todo en uno". El PVA permite controlar el tamaño de partícula de Ni aumentando su dispersión y por tanto el número de centros activos. En este trabajo, se usarán los polímeros PVA, polivinilpirrolidona (PVP) y polietilenglicol (PEG) para aumentar la dispersidad y, por tanto, tener más centros activos.

LABURPENA

Lan honetan polimero ezberdinek (edo polimero berdina propietate ezberdinekin) ur gehiegizko bustitze heze bidez prestatutako Ni-La/Al_2O_3 katalizatzaileetan sortzen duten eragina aztertzea da. Hori lortzeko katalizatzaileak "Dena batera" metodoa erabiliz prestatu ziren, gure laborategiko taldean garatutako metodo bat. Metodo hau bukaerako katalizatzailea lortzeko osagai guztiak (euskarria, material aktiboaren gatz aitzindaria eta gehigarriak, non polimeroak sartzen diren) nahasten dituen suspentsio baten sorreran oinarritzen da. Metodoak substratu egituratuak zuzenean gainezartzeko erabiliko diren katalizatzaile suspentsioak prestatzeko ahalmena ematen du, eta, baita ere, suspentsio hauek lehortu eta kaltzinatu ondoren, karakterizazio tekniketan erabiliko den suspenditutako katalizatzaileak hauts moduan prestatzeko balio du.

Egindako suspentsioak biskosimetria bidez karakterizatu ziren, honela, polimero ezberdinek biskositatean zuten eragina ikusteko, ondoren, suspentsioak lehortu eta kaltzinatzean, lortutako suspenditutako katalizatzaileak karakterizatzeko teknika ezberdinak erabili ziren: N_2 fisisortzioa, CO-ren kimisortzioa, tenperaturaren erredukzio programatua (TPR) eta X-izpien difrakzioa. Karakterizazio hau katalizatzailera gehitutako polimeroak sortutako eraginak aztertzeko erabili ziren, Sabatier-en erreakzioetarako onuragarria izan beharko lukeena. Lortutako emaitzak, formulazioan erabilitako polimeroaren arabera aldatzen ziren, katalizatzailearen eraginkortasuna aldatuz, baita, polimero berdina erabiliz, pisu molekularra eta hidrolisi maila aldatuz, emaitza ezberdinak lortzen ziren, polimero batzuen erabilgarritasuna hobea izanik.

Bestalde, aurkitu izan zen polibinil alkohol (PVA) eta nikelaren erabilera zuzenean eragiten zuela "Dena batera" metodoarekin prestatutako katalizatzaileen propietatetan. PVA-k nikelaren partikula tamaina kontrolatzeko balio du, azkeneko honen dispertsioa handituz eta beraz zentro aktibo kopurua. Lan honetan PVA, polibinilpirrolidona (PVP) eta polietilenglikola (PEG) polimeroak erabiliko dira dispertsio hori handitzeko eta, beraz, zentro aktibo gehiago lortzeko.

1. INTRODUCTION

1.1. CLOSED CARBON CYCLE

The carbon element is basically the founder of all life on earth, indispensable for the formation of complex molecules like proteins or DNA. Also found in the atmosphere in the form of carbon dioxide (CO_2), carbon helps to regulate Earth's temperature, make all life possible or being a key ingredient in the food that sustains us, also provides large quantities of energy to fuel our economy.

The closed carbon cycle describes the process in which carbon, with no interruptions, travels from the atmosphere to the Earth and then back to the atmosphere (Figure 1). Since our planet and its atmosphere have a closed environment, the quantity of carbon will not vary. Wherever the carbon is located (in the atmosphere or on Earth), is constantly in flux. [1]

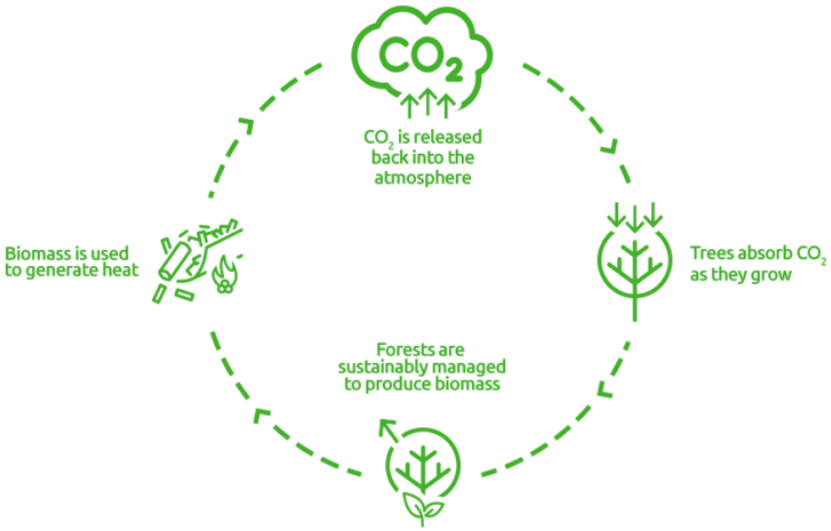

Figure 1. Closed carbon cycle. [2]

The obtained biomass from this closed carbon cycle can be used as fuel in order to substitute the fossil fuels used nowadays, but why is it that? Although in a combustion process biomass is burnt and cannot be recovered, it is considered a renewable energy source such as wind or solar energy, but why is not considered in the same group of fossil fuels?

This is because the CO_2 burned in the combustion of fossil fuels was locked underground millions of years ago, the releasing of that CO_2 affects the balance of carbon in the atmosphere. However, biomass is carbon neutral, the plants absorbs carbon with the process of photosynthesis which is released during the combustion process. Therefore, combustion of biomass offsets CO_2 emissions, being part of the close carbon cycle (Figure 1) it net emissions are zero.[3]

Nowadays, the main quantity of energy is obtained from fossil fuels, which makes a total demolition of the closed carbon cycle system. Using the fossil fuels, the quantity of CO_2 entering the atmosphere is highly dangerous due to the problems the accumulation of this gas can cause, some of the most well-known are: carbon footprint or global warming.

The closed carbon cycle prevents huge quantities of CO_2 from entering the atmosphere, in order to achieve that, far-reaching changes are required, such as the way we generate electricity or heating energy, or the energy provided for industries or mobility. Furthermore, methods for energy production or CO_2 storage must be developed, new technologies must also be politically enforceable and accepted by the public.[4]

1.2. NATURAL GAS

Natural Gas (NG) presents an important role in the actual energetic system, mainly used as a fuel to generate electricity and heat. It is a mixture of gases, including methane, small quantities of ethane, propane, butane and superior hydrocarbons such as CO_2, H_2S and noble gases (helium). Natural Gas reserves are deep inside the earth near other solid or liquid hydrocarbons beds like coal and cruel oil. [5, 6] It can be transported to long distances efficiently through enormous pipes and is distributed to industries and homes through local pipes system (Figure 2).

Figure 2. Natural gas pipes system in Spain (2015).[7]

Natural Gas is a fossil fuel that does not contain as much heavy metal as gasoline or coal has, also the sulphuric components can be easily moved away efficiently to really low levels using the technology of elimination of acidic gases. As the methane is the principal component of Natural Gas, the carbon footprint leaved after its incineration is the smallest among the hydrocarbons, due to the hydrogen rate per carbon is the lowest one, H:C of 4. In addition, Natural Gas possess a higher energy density than the hydrogen, which means an easy and fast transport of huge energy quantities with an insignificant loss of load.[8]

Natural Gas has become the favourite fuel for the generation of electric energy among the developed countries (Figure 3), due to its low contamination rate, the small capital cost compared with the coal electric factories and the improvement on the technology of gas turbines.[8] Moreover, Natural Gas is the best-liked raw material for the production of hydrogen in the industrial area. Approximately, according to the Energy Information Administration of the U.S. Government, natural gas consumption in 2003 occupied a quarter of the total demands of raw materials among the developed countries, increasing day after day.[9, 10]

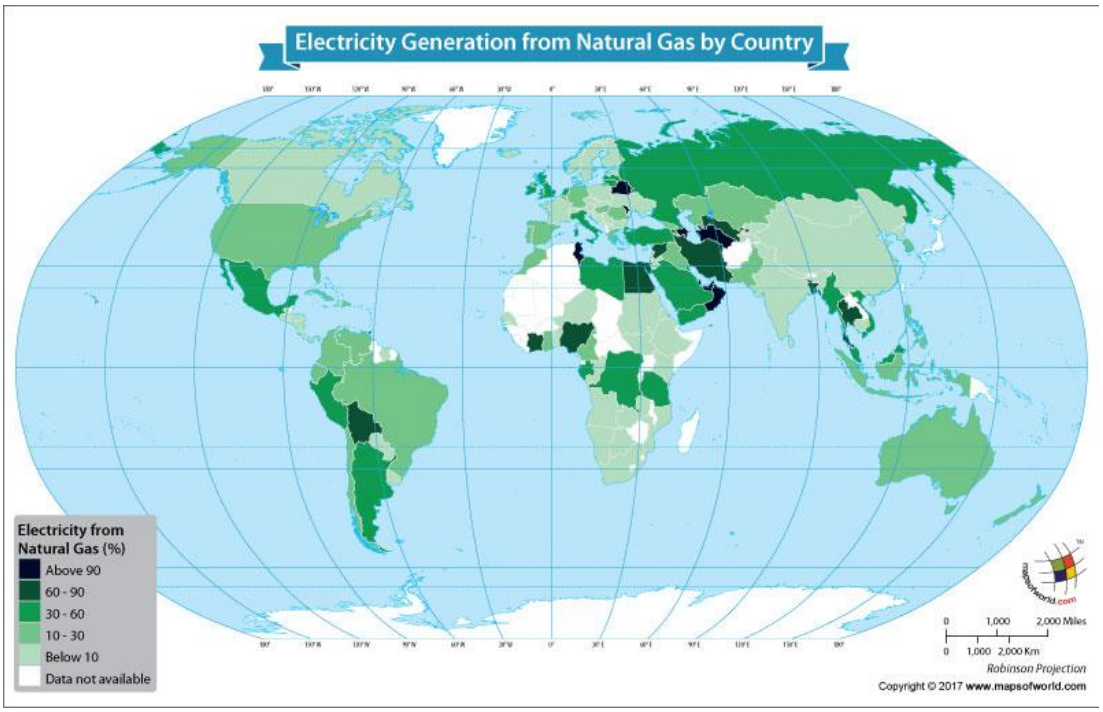

Figure 3. World electric generation from natural gas (%) in 2017.[11]

Natural Gas plays an important role as energy source worldwide. The production of Substitute Natural Gas from biomass (Bio-SNG) is an attractive option to reduce CO_2 emissions and replace declining fossil Natural Gas reserves, as a consequence, it has gain both, the politic and public support, in the majority of the countries, as it is proved in the effort made to recycle the biomass from sewage treatment plants, dumping sites, plants for the treatment of municipal waste, etc. The obtained Bio-SNG, also known as green gas, plays an essential role in the objective of getting renewable energy in Europe.

The process of methanation of biomass by anaerobic fermentation and the thermochemical methanation of biomass by gasification are nowadays the conversion processes commercially exploded. In contrast to the processes by fermentation, that have the capacity of small-medium productions (1-10 MWt), the gasification method allows to make conversions at high scales (50 MWt).[12, 13]

In both cases, the CO_2 is an important by-product of the conversion of the biomass, about 40-50% for the fermentation and at least 50% for the gasification. Nowadays, CO_2 is eliminated in order to maintain the correct specifications of the Bio-SNG, what takes energetically expensive processes of separation. Nevertheless, in the case of gasification, the resulting gas contains H_2 and CO, which requires a final step of

thermochemical methanation for the fabrication of sufficiently pure methane to inject it into the gas net. The production cost of the Bio-SNG from the biomass, even with the improvements in technology of the last generations, continues being significantly higher than the production from Natural Gas. The principal expenses come from the inversions on the gasification or the equipment upgrades, also from the relatively high cost of biomass. However, the Bio-SNG produced from biomass is a renewable fuel which can be distributed around the whole energetic system, what makes it a promising carrier of renewable energy.[14]

Taking into account that the gas obtained in the gasification has a high quantity of CO_2, an alternative would be the addition of H_2 in order to eliminate the carbon dioxide and produce additional methane. In this case, the CO_2 would be considered as raw material vital for the renewable energy companies, and not as an industrial waste product.[15] The production of Natural Synthetic Gas (Bio-SNG) from the electrolytic production of hydrogen and the methanation with CO_2 makes the obtained Natural Gas totally renewable. This technology is known as *Power to Gas* (Figure 4). However, it is not sufficiently developed to take and transform entirely the electric and gas nets.[16]

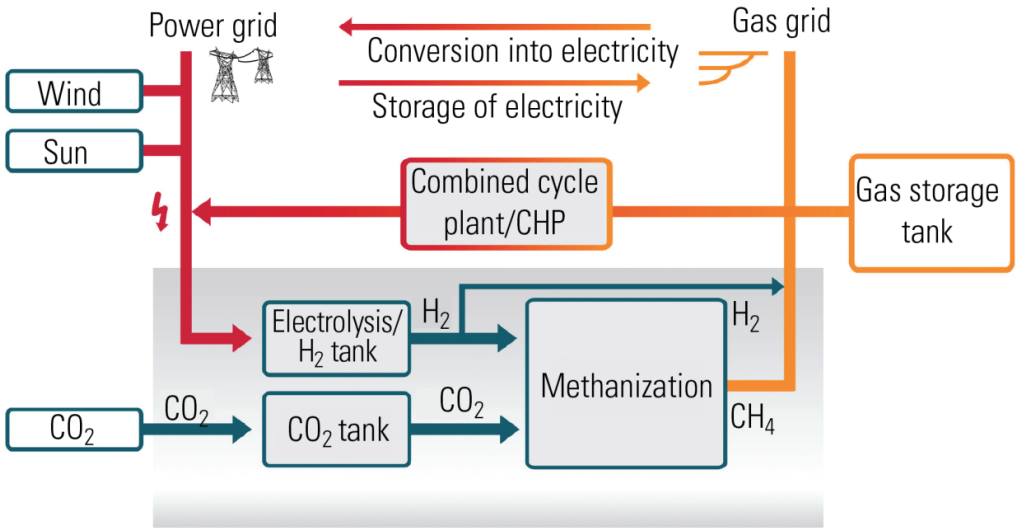

Figure 4. *Power to Gas* technology.[17]

The design of efficient processes for the production of SNG requires the development of conversion processes effective for the creation of H_2 from electric energy, conversion of CO_2 and H_2 to SNG and also an infrastructure that guarantees a high efficiency and flexibility.

1.3. SABATIER REACTION

The basis for the *Power to Gas* process is a promising reaction known as Sabatier Reaction (see Equation 1), where methane (CH_4) is obtained from the conversion of carbon dioxide (CO_2) and hydrogen (H_2). Nowadays carbon dioxide is obtained for fossil fuels, but it can also be obtained from biogas, syngas, or other industrial processes of air, resolving one of the greatest environmental threats of our times, global warming.[6, 18]

$$CO_2 + 4H_2 \rightarrow CH_4 + 2\,H_2O \qquad \text{Equation 1}$$

The produced methane is a safe gas which can be used for the generation of electricity or energy for internal combustion engines, also for the generation of biodiesel or other hydrocarbons. The process is economical due to the low energy requirement respect other processes such as carbon capture and storage (CCS) systems that requires fossil fired power plants, large facilities and high energy imputs.[19, 20, 21]

The methanation of CO_2 is highly exothermic reaction ($\Delta H^0_{298,15K}$ = -164.63 kJ/mol), thermodynamically favoured (ΔG^0= -131 kJ/mol) and kinetically unfavoured. It occurs at high temperatures, around 200 °C in presence of catalysts. However, due to the increase of the by-product CO at higher temperatures, the studies of the reaction are commonly done from 200 to 500 °C. For the methanation of CO_2, showing good catalytical performances, heterogeneous catalysts are used, the most famous ones based on Rh, Ru, Pd and Ni. Ni-based catalysts, as a result of their high activity, high selectivity and low cost, are the most widely investigated materials.[22]

The major downsides of the Ni-based catalysts in Sabatier reaction are the high temperature and high operating pressures that influence directly in carbon formation. At atmospheric pressure, carbon may be formed by three different reactions, including Boudouard reaction ($2CO \rightarrow C + CO_2$), reduction of carbon dioxide ($CO_2 + 2H_2 \rightarrow C + 2H_2O$) and reduction of carbon monoxide to carbon ($CO + H_2 \rightarrow C + H_2O$). The nature and properties of the support have also a major role in the catalytic performance of Ni-based

catalysts, strongly influencing the dispersion of the catalyst active phase, the metal-support interaction and the reducibility of the metal oxide precursor. Linked with Ni-based catalysts, the most investigated supports are γ-Al_2O_3, SiO_2, CeO_2, ZrO_2 and some mixed oxides such as CeO_2-Al_2O_3 or CeO_2-ZrO_2.[22]

Ni supported on inorganic oxides catalysts are commonly prepared by wet impregnation and use to have three different parts, the support, the active phase and a promoter, this last takes the responsibility of helping the active phase to reduce. The support must have a large surface and a well porous distribution in order to disperse the active phase as good as possible, looking forwards to obtain a large distribution of the active phase with a small particle size.[23]

On previous lab works made in our laboratory group, for example the one made by Nerea Sánchez Guerra, the structuring of the catalysts Ni/La-Al_2O_3 for the production of the Synthetic Natural Bio-gas was studied (see reference 6).

The catalysts were prepared with the "All in one" method, which makes viable to create suspensions containing everything necessary for the final catalysts. Those suspensions can be used directly for coating of structured substrates or, after drying and calcinating them, as slurried catalysts in powder form.

She demonstrated that the addition of polyvinyl alcohol (PVA) to the formulation of the catalysts improved the controlling of the particle size of the nickel. The importance of this remains on the dispersion obtained with different sizes, which affects directly to the quality of the catalysts. The conclusion obtained was that the catalysts can be improved by adding polymeric surfactants, causing a decrease in the particle size of the Ni and, as a consequence, the scatter is larger and the creation of active centres increases.

1.4. PREPARATION OF IMMOBILIZED NANOPARTICLES ON SOLID SUPPORT

The creation of supported metallic samples based on the deposition of metallic nanoparticles on solid support preformed in solutions (colloids or sols) is called sol immobilization. The advantage of this technique is that the particle size is controlled with a narrow size distribution. Metallic colloids are obtained in the presence of stabilizing or capping agents by the reduction of a metal precursor in solution.

There are several disadvantages when talking about the application of liquid suspensions of metal nanoparticles in catalysis. In fact, using this system, the separation of the products and the recycling of the catalyst are limited. Nevertheless, as a consequence of the adsorbance of other stabilizers and salts, killing catalytical activity, the supported nanoparticles are generally less satisfactory.

For the immobilization of metal colloids numerous immobilization methods and several supports have been investigated. Transition metal nanoparticles can be chemically bonded to polymeric support or adsorbed on inorganic support.[24] Based on the stabilizing agents used, there are four distinguished stabilization procedures: the Electrostatic stabilization by the surface adsorbed anions, the Steric stabilization by the presence of bulky groups, the combination of the previously mentioned stabilizations with the Electrosteric stabilization as surfactants, and finally the stabilization with a ligand.

Electrostatic stabilization can be generated when ionic compounds such as halides, carboxylates or polyoxoanions are dissolved in solutions (generally aqueous). The adsorption of those compounds and their respective counterions on the metallic surface will generated an electrical double-layer around the particles (Figure 5) and, as a consequence, will result in a Coulombic repulsion between particles preventing particle aggregation if the electric potential associated with the double layer is high enough.[24]

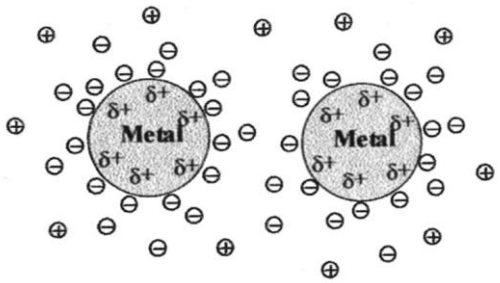

Figure 5. Schematic representation of electrostatic stabilization of metal colloids particles.[24]

Steric stabilization happens when macromolecules such as polymers or oligomers are used to prevent metal colloids from aggregating. The adsorption of those molecules will create once again a protective layer which will prevent the mentioned aggregation. This can be easily explained using Figure 6, where it can be seen that the adsorbed molecules will be restricted in motion causing a decrease in entropy and so an increase in free energy.[24]

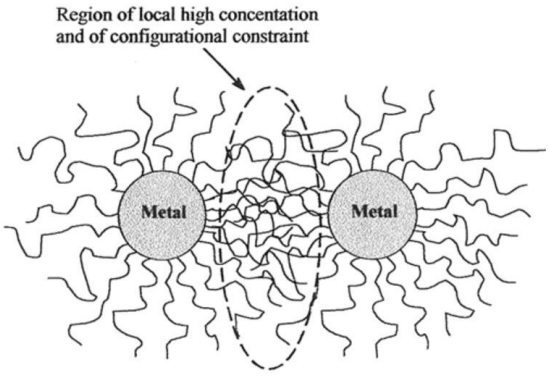

Figure 6. Schematic representation of steric stabilization of metal colloids particles. [24]

Both techniques can be combined to maintain metallic nanoparticles stable in solution, creating the stabilization procedure known as Electrosteric stabilization. This type of stabilization is generally provided through ionic surfactants. These compounds carry a polar head group who is able to create an electric double layer and also a lipophilic side chain able to maintain the steric repulsion.

Finally, the stabilization by a ligand or a solvent occurs simply by the coordination of metallic nanoparticles with ligand such as phosphines, thiols, amines or carbon monoxide. [24]

The agents added to the solution can also be micelles formed with diblock copolymers or surfactant, and dendrimers (Figure 7). The objective is to control the growth of the particles during the reduction, avoid aggregation and precipitation. Reduction is usually performed by addition of a chemical agents such as those mentioned earlier, sodium borohydride, hydrazine or weaker reducing agents such as amine-borane complexes, methanol or glucose.[25]

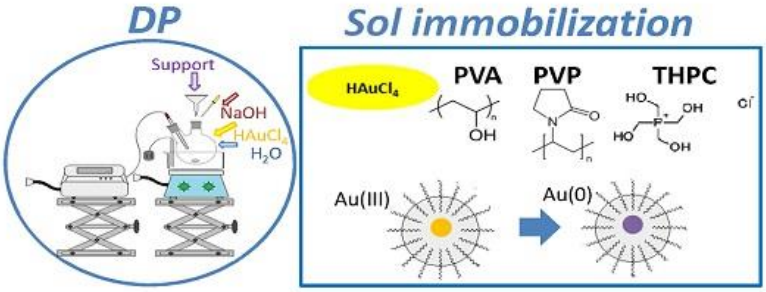

Figure 7. Preparation of gold nanoparticles with the sol immobilization technique.[25]

However, in Nerea Sanchez Guerra´s final degree project it was demonstrated that sol immobilization method without reduction step and removing the PVA completely by calcinating a higher dispersion of the active phase could be obtained and consequently a decrease on the particle size of the nickel oxide supported (Figure 8). Therefore, it can be said that the steric stabilization with PVA is effective for heterogeneous catalysts preparation.

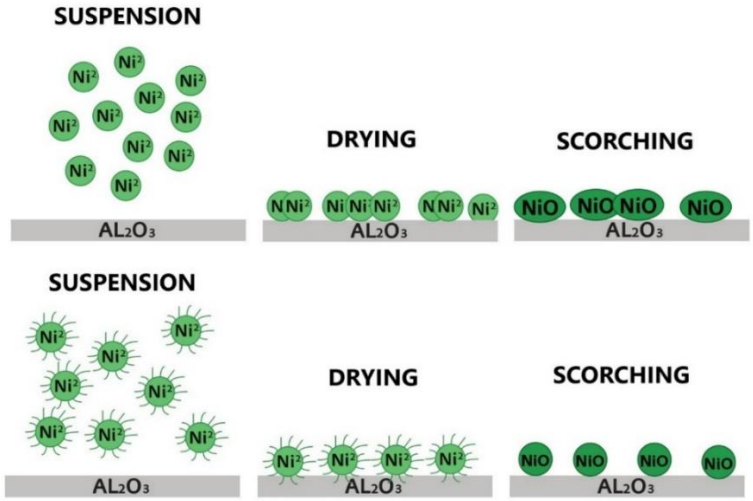

Figure 8. Outline of every step without PVA (up) and with PVA (down).

1.5. THE OBJECTIVE

The principal objective of this work will be to examine the effects different polymeric surfactants with variations on their molecular weight and hydrolysis degree can have in the Steric stabilization for catalysts prepared to use into Sabatier's reaction. The prepared suspensions will be characterized by viscosimetry, and after drying and calcinating them, the obtained slurried catalysts in powder form will be analysed with different characterisation techniques: N_2 physisorption, CO chemisorption, temperature programmed reduction and X-ray diffraction.

For the preparation of aqueous suspensions and slurried catalysts, the method "All in one" will be used, a method which includes every component for the readying of the catalyst: the support, the precursor salt of the active material and the additives, were polymers are introduced.

2. EXPERIMENTAL PART

2.1. PREPARATION OF THE CATALYSTS

The method used for the preparation of every catalyst was the "All in one" method. This method consists on the readying of an aqueous suspension which includes every component necessary for the preparation of the future catalyst: the support, the precursor salt of the active material and the additives.

This method was developed in our laboratory group and able us to prepare a suspension of the catalyst which can be used with no hesitation as catalyst powder (after drying and calcinating it) or used directly for the coating of structured substrates.[26]

To prepare the catalysts, different quantity of the following reactants were mixed:

- Nickel (II) nitrate hexahydrate [$Ni(NO_3)_2 \cdot 6H_2O$; Sigma-Aldrich]
- 3% La-Al_2O_3
- Polymeric surfactants [Polyvinyl alcohol (PVA), polyvinylpyrrolidone (PVP), polyethylene glycol (PEG)] (Table 2)
- Colloidal Alumina [AL20; Nyacol Nano Technologies, Inc.]
- Distilled water.
- HNO_3 for the adjustment to pH=4

To obtain La-Al_2O_3, the alumina (Spheralite) available at the laboratory, which was storaged in shape of pellets, was transformed in alumina powder using a disc mill (transformation of sizes from 2 mm to 10 μm). In order to get the needed La-Al_2O_3 pore impregnation technique was used. The technique consisted on spraying the alumina powder with a previously prepared solution of $La(NO_3)_3 * 6H_2O$ in a continued stirring.

To prepare 500 g of La-Al_2O_3, 46.7595 g of $La(NO_3)_3 * 6H_2O$ with 188.337 mL H_2O are needed. In this case 463.60 g of lanthanum alumina were prepared, what required 43.3573 g of $La(NO_3)_3 * 6H_2O$ and 174.626 mL of water. After obtaining the La-Al_2O_3 the final step was the drying the powder (120 °C for 24 h) and calcination (900 °C for 6h with a ramp of 5 °C/min)

The procedure for the preparation of all the catalysts was the same. The only change was the polymer used in each suspension. The formulation used in each catalyst with this method is shown in Table 1.

Table 1. Formulation used for the preparation of the catalysts.

Reactants	Quantity (g)
Distilled water	129.34
Polymer	1. 4708
$Ni(NO_3) \cdot 6H_2O$	9. 9095
3% La-Al_2O_3	10. 6021
Nyacol	1. 6035

As said, different polymers were used for the preparation of the catalysts, which are shown in the following Table 2.

Table 2. Polymers used for the preparation of the catalysts.

Polymer	Brand	MW (mol wt)	Code
PVA-Mowiol 4-88	Sigma-Aldrich	31000*	81381-1KG
PVA-Mowiol 5-88	Kuraray	37000*	-
PVA-Mowiol 13-88	Kuraray	69500**	-
PVA-Mowiol 23-88	Kuraray	92200	-
PVA-Mowiol 25-88	Kuraray	92600**	-
PVA-Mowiol 47-88	Kuraray	138900**	-
PVA-Mowiol 28-99	Sigma-Aldrich	145000*	10849-1KG
PVA-Mowiol 4-98	Sigma-Aldrich	27000*	81382-1KG
PVP 10000	Sigma-Aldrich	10000*	PVP 10-500G
PVP 40000	Sigma-Aldrich	40000*	PVP 40-50G
PVP 360000	Sigma-Aldrich	360000*	PVP 360-100G
PEG 2000	Sigma-Aldrich	1900-2200*	84797-250G-F
PEG 3350	Sigma-Aldrich	3015-3685*	202444-250G

*MW obtained from the polymer datasheet

**MW obtained from articles[26]

For the readying of the catalysts with the method "All in one" the coming procedure was followed:

- First, the polymer was dissolved in distilled water with the magnetic stirring. Depending on the polymer added the bain-marie was used, heating the distilled water up to 80 ^{o}C. Once the polymer was dissolved, the solution was cooled to room temperature.
- Next, the proper amount of Nickel (II) nitrate hexahydrate [Ni $(NO_3)_2 \cdot 6H_2O$] was added.
- Afterwards, the support (3% La-Al_2O_3) was added gently, if it is introduced too fast the support will not scatter correctly.
- Once all the support was dispersed, the colloidal alumina (Nyacol) was added with the purpose of improving the adhesion to the metallic substrate.
- Finally, the pH was adjusted to 4 using concentrated HNO_3 and left the suspension resting for 24 hours.

Later, with a view to get the catalyst dust, the suspensions were dried using a bain-marie and a magnetic stirring. As soon as obtaining a kind of viscous liquid it was dried in a muffle furnace for 12 h at 120^{o}C. To conclude, the samples were calcinated for 2 h at 500 ^{o}C (5 ^{o}C/min).

2.2. CHARACTERISATION OF THE CATALYSTS

2.2.1. Viscosity

The viscosity is defined as the resistance a material makes when it flows, which is an important factor in coating. When that resistance is low, the fluid has small viscosity and otherwise, when that resistance is high, the fluid is viscous.[27, 28]

The viscosity was measured in each of the suspension prepared with the method "All in one" with a rotational rheometer, also known as a rheometer $AR1500_{ex}$ of the brand TA instruments. The geometry used for every measurement was cylindrical, with a diameter of 28 mm. The calculations were made between two cycles in which the rotational speed changed, with regard to the shear rate, this was measured between 0 and 3600 s^{-1}.

2.2.2. Zeta potential

Zeta potential is a physical property which is exhibited by any particle in suspension, macromolecule or material surface. With its measurement the stability of solid suspensions or the stability of colloidal scattering can be determined. It can be also used to predict interactions with surfaces, and optimise the formulation of films and coatings.[27]

When a solid material is immersed in a dispersed environment, its surface interacts with the molecules of that environment, this way a balance between repulsive and attractive forces will be created. The stability of the dispersions will be determined with the interactions between the solid particles. The colloidal system will be stable if the particles have a sufficiently high repulsion. However if a repulsion mechanism does not exist then flocculation or coagulation will eventually take place.[27, 29]

The dispersion environment used was water, it is important to know the behaviour of the support in order to prepare stable catalytic suspensions. In aqueous media, the pH of the sample is one of the most important factors that have an effect in zeta potential. Depending on the pH, the outer layer of the solid will charge positively or negatively. For example, if more alkali is added to the suspension, the particles have a tendency to acquire more negative charge.

The charge can increase or decrease, there will be a point where the charge is equal zero, at this moment the isoelectric point will be reached (Figure 9). At this point, there will not be any type of repulsive forces and, as a consequence, particle aggregation will happen. To measure the surface charge, a feature that only appears in those solids who have electrically charged skin is used. Zeta potential cannot be measured directly, but knowing that it is proportional to the speed of particles when an electrophoretic movement happens, it can be estimated.

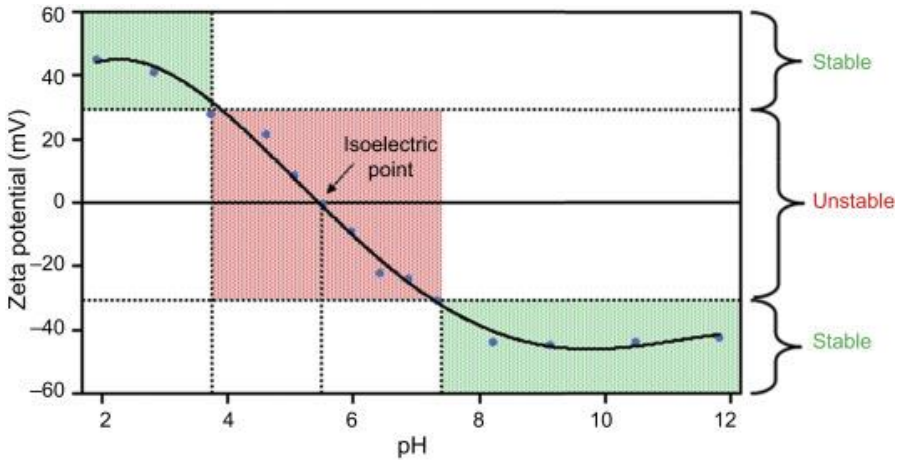

Figure 9. Zeta potential representation.[30]

In order to measure the zeta potential 6 samples were prepared with different pH (2, 4, 6, 8, 10 and 12). Samples were prepared using 20 mg of La-Al_2O_3 and 50 mL from a solution of NaCl with a concentration of 3 mM. To adjust the pH, HNO_3 and NH_4OH were used. After, the samples were introduced in a Bandelin (Sonores digitec) ultrasound machine for an hour with a constant temperature and finally maintained 24h in orbital shaking. To conclude, pH was checked and Zeta potential was determined using a machine model ZetaSizer of Malvern Instrument.

2.2.3. Measurement of particle size by laser diffraction

Diffraction is known as the slight bending of light as it passes around the edge of an object. The relative size of the wavelength of light to the size of the opening has a notable effect on the amount of bending. The bending will be almost unnoticeable if the opening is much larger than the light's wavelength. However, bending will be considerable, even easily seen with the naked eye if the two are closer in size or equal.[31] With this technique the distribution of particle size of a solid can be determined when it is dispersed in liquid, supposing that those particles are not added.[32, 33]

The equipment to analyse the samples was a Mastersizer 2000 of Malvern Instruments. The samples were prepared dispersing 100 g of La-Al_2O_3 in 20 mL of distilled water, which was previously adjusted to pH=4 because the curve shows that the suspensions are stable at that pH. Subsequently, samples were introduced into ultrasound for 2 h at room temperature (maintaining the temperature constant to avoid

particles aggregations). Finally, samples were tripled and analysed using an average of 3 mL for each one.

2.2.4. SEC-MALS

In order to measure the molecular weight of some polymers used in the lab work, SEC-MALS was used, which combines the multi angle light scattering with size exclusion chromatography. It is a very advanced technique for characterization of macromolecules in terms of molar mass, size or even conformations. The SEC column serves to separate the introduced molecular by hydrodynamic volume; in contrast with basic GPC, the retention time is not used to determine the molecular weight of the samples. After exiting the columns, the molecules pass through a MALS detector and are probed by a laser beam. The obtained MALS signals, along with the differential refractive index signals are analysed to obtain the needed physical properties of the molecules. [34]

SEC-MALS was used in order to find the absolute molar mass of the polymers. For that, the samples where characterized using different fractionation techniques, size exclusion chromatography (SEC) coupled with a multiangle light scattering (MALS) and a refractive index (RI) detector. The SEC/MALS/RI data was analysed by using the ASTRA software version 6.0.3 (Wyatt technology, USA). The absolute molar mass was calculated from the MALS/RI data using the Debye plot (with the first order Zimm formalism).[35] Debye plot was obtained on the basis of the Equation 2,

$$\frac{K*c}{R(\theta)} = \frac{1}{MwP(\theta)} + 2A_2c \qquad \text{Equation 2}$$

where the axis x would be the concentration and the axis y K*c/R(θ).[36]

The objective of this technique was to find the absolute molar mass of the polymers, but only the one for Mowiol 47-88 was found. However, it is an indispensable technique for the characterisation of the catalsyst.

2.2.5. Physisorption of N_2

Also known as physical adsorption, is a process in which the electronic structure of an atom or molecule is barely perturbed upon adsorption. [37, 38] It allows obtaining textural information related not only with the specific surface of the solid (m^2/g_{solid}), but also with its porous structure (pore volume, average pore size, etc.).

The adsorption is given by weak interactions among the gas and the outer layer of the solid, known as physisorption, is caused by *Van der Waals* forces. These interactions are only possible if the surface of the solid is free from other probable adsorbed molecules and if it is favoured by the pressure. This way, if there is an increase on the pressure of the gas that has been introduced, the quantity of the gas that is absorbed grows up to a saturation value in a determined temperature. This is the cause for the creation of isotherms of adsorption.

The process is reversible due to the interaction between molecules, *Van der Waals*, with the objective of obtaining more information about the textural properties, vacuum has to be applied after the adsorption to get isotherm of adsorption-desorption.

The textural properties previously mentioned are obtained for the isotherm and the application of the corresponding mathematical expressions. The model *Brunauer-Emmett-Teller (BET)* is used to calculate the specific surface, and the variant *Barett-Joyner-Halenda (BJH)* to get the distribution of pore size. [27, 39]

For the analyse of the slurried catalysts a machine model Micromeritics ASAP 2020 was used. Approximately 200 mg of solid dust is weigh, to which previously a degassing is applied in 180 ^oC until the vacuum reaches 100 µmHg. Afterwards, the adsorption of N_2 (Air liquid, 99.999%) is done at the saturation temperature of liquid N_2 (77 K), where the gas it is adsorbed at relatively low pressures, first in the most energetic region and next in the lower energetic region.

2.2.6. Chemical adsorption or chemisorption of CO

Chemisorption is a kind of adsorption which involves a chemical reaction between the surface and the gas molecules, adsorbing on specific locations, known as active centres (Figure 10). This technique is useful for evaluating physical and chemical properties of materials that are critical for process / reaction performance to measure the quantity of active centres and, as a consequence, the active surface of the catalyst. Chemical adsorption is an interaction much stronger than physical adsorption, in fact, the interaction in this technique is an actual chemical bond where electrons are shared between the gas and the solid surface, also known as covalent bonding. Due to the type of bonding in this technique, contrary to physisorption, the process is irreversible.[37, 40]

Primarily chemisorption is used to evaluate the number of active centres, but can also be used to measure the temperature at which catalyst become active, strength of specific types of active sites, or ability of materials to perform after reduction/oxidation cycles.

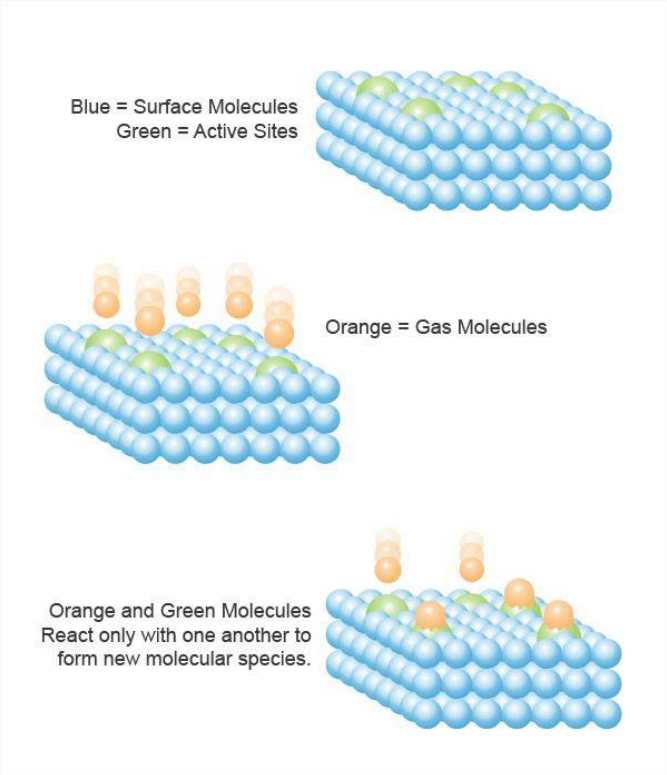

Figure 10. Process of chemisorptions.[41]

Chemisorption allows measuring the dispersion, the metallic surface and estimating the particle size measuring the outer layer of the metal adsorbed in the surface of the support. Metallic dispersion (D) is calculated with the Equation 3. Once the chemisorption is done, the sample has to be heated up to high temperatures in order to guarantee the quantitative oxidation of the reduced fraction, the consumed oxygen is measured to determine the reduced fraction (R) of the catalyst (Equation 4).

$$D\ (\%) = \frac{number\ of\ surface\ metallic\ atoms}{total\ number\ of\ metallic\ atoms} \cdot 100 \qquad \text{Equation 3}$$

$$R\ (\%) = \frac{number\ of\ reduced\ atoms}{total\ number\ of\ metallic\ atoms} \cdot 100 \qquad \text{Equation 4}$$

The analysis where made with a Micromeritics ASAP 2020 C equipment. An average of 200 mg of catalyst where introduced in a quartz cell and followed the steps on the next Table 3:

Table 3. Steps of chemisorption by CO.

Task number	Task name	Gas	Temperature (°C)	Rate (°C/min)	Time (min)
1	Flow	He	120	10.0	10
2	Evacuation	He	120	10.0	120
3	Flow	H_2	550	2.0	300
4	Evacuation		550	10.0	90
5	Evacuation		35	10.0	60
6	Leak Test		35	10.0	
7	Evacuation		35	10.0	60
8	Analysis	CO	35	2.0	

The stoichiometry of the used adsorption was CO:Ni = 1:1.

With the objective of finding the grade of reduction of the catalyst, a process of oxidation was design after the chemical adsorption. In this case, the steps that were followed are showed in the coming Table 4:

Table 4. Steps of the oxidation.

Task number	Task name	Gas	Temperature (°C)	Rate (°C/min)	Time (min)
1	Evacuation		100	10.0	60
2	Flow	He	100	5.0	5
3	Flow	He	400	5.0	90
4	Evacuation		400	5.0	120
5	Leak Test		400	5.0	
6	Evacuation		400	5.0	90
7	Analysis	O_2	400	5.0	

The procedure followed for the preparation of the dust catalysts was the same in physisorption and chemisorption, but in this last adsorption the tube was different, with a diameter of 12 mm, a quartz tube was used (Figure 11).

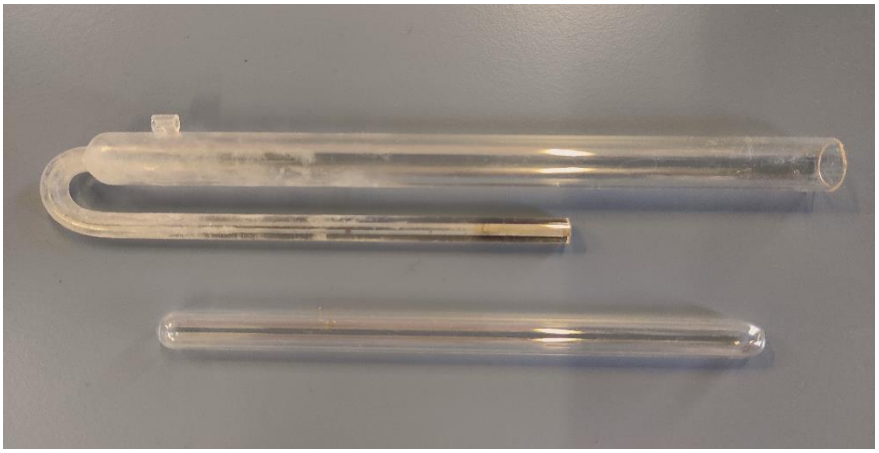

Figure 11. Quartz tube used for chemisorption.

2.2.7. Temperature-programmed reduction (TPR)

Temperature programmed reduction (TPR) is a widely used tool for the characterisation of metal oxides, mixed metal oxides and metal oxides dispersed on a support. This method yields quantitative information of the reducibility of the oxide's surface, the heterogeneity of the reducible surface or the redox behaviour of the

catalyst. TPR includes a reducing gas mixture (typically Hydrogen diluted in argon or nitrogen) and an inert gas (Ar, He), both gases flowing over the sample (Figure 12). When the sample is suppress to a controlled thermal treatment, normally being a warming at a constant speed in a regulated atmosphere, the centres react to reduce.[42]

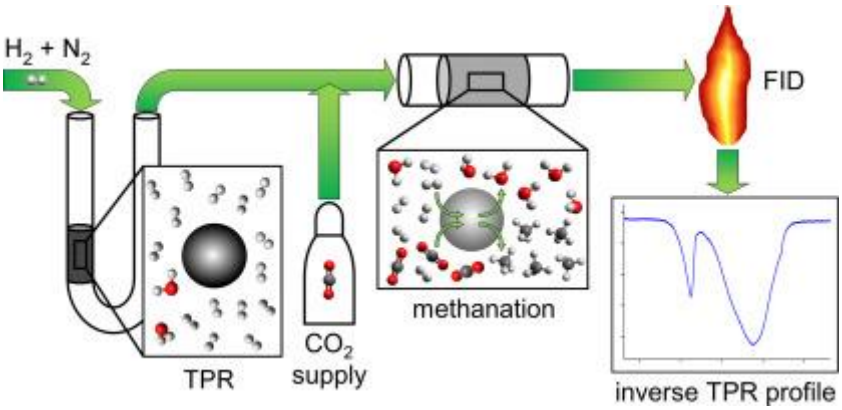

Figure 12. New methodical approach for TPR.[43]

A thermal conductivity detector (TCD) is used to monitor the changes in the thermal conductivity of the gas stream. The TCD signal is converted when the adequate conditions to happen the reduction are reached, while the fed gas consumes. The area of the obtained curve is proportional to that of the total mass reduced, taking this into account the total reducibility of the sample can be measured. The TPR can be also used to determine the ideal temperature for the reduction of the catalyst, which coincides with the maximum of the graphic.[42]

2.2.8. X-ray diffraction (XRD)

The atomic planes of a crystal cause an incident beam of X-rays to interfere with one another as they leave the crystal, this is known as X-ray diffraction. X-ray diffraction can be used to identify the crystalline phases of the catalysts, which can lead to obtain crucial crystallographic data.[44] The information is collected in a diffractogram and it has to be compared with pure substances diffraction patterns, this way different phases of the compounds can be known. The technique can be also used to measure the crystal size between 2 and 50 nm.

X-ray diffraction is based on constructive interference of monochromatic X-rays and a crystalline sample. The X-rays are generated in a cathode ray tube by heating a filament to produce electrons, accelerating the electrons towards a target applying a voltage and directing those electrons to the sample. X-ray spectra is produced when electrons have sufficient energy to dislodge inner shell electrons of the target material. The interaction of the rays with the material produces constructive interference when conditions satisfy Bragg's law (Equation 5).

$$n \times \lambda = 2 \times d \times sin\vartheta \qquad \text{Equation 5}$$

This law relates the wavelength (λ) of electromagnetic radiation to the diffraction angle ($sin\vartheta$), the lattice spacing in the crystalline sample (d) and the order of the diffraction (n). (Figure 13)

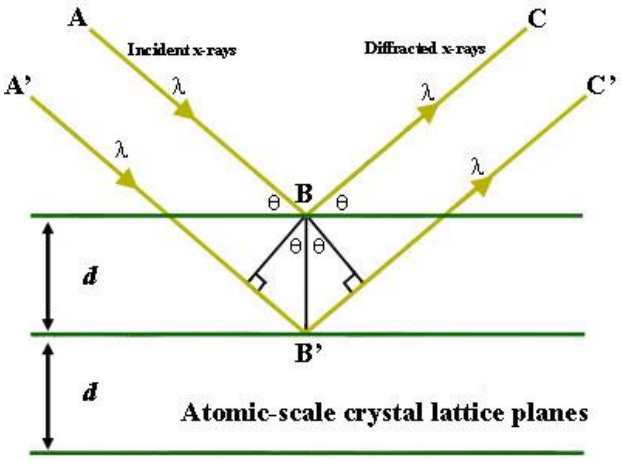

Figure 13. Bragg's law representation.[45]

The diffractograms of the catalysts were obtained in a machine Bruker D8 Advances with monochromatic radiation (40 kV/30 mA) of Cu K_α, λ =0.154 nm with a graphite monochromator and an automatic slit. The data was collected with values of 2ϑ between 10 and 90° with steps of 0.05 ° and 12 s for each step.

The XRD technique was used to estimate the average crystal size of the Ni catalysts. To achieve that, the most intense peak of the graphic was taken into account, 2ϑ between 40 and 50 º with steps of 0.02 º and 25 s per step. The crystal size was determined using Scherrer equation (Equation 6):

$$\tau = \frac{k \times \text{of } 2\vartheta}{\beta \times cos\vartheta} \qquad \text{Equation 6}$$

Where K=0.9 the factor of form, which depends on the used machine, λ=0.154 nm is the wavelength of the X-ray source, β is the width of the peak at middle height and ϑ, the angle where is located the strongest peak.

3. RESULTS

In this part, the results obtained for the different catalysts suspensions and slurried catalysts from each characterization technique will be presented.

3.1. ZETA POTENTIAL AND PARTICLE SIZE

With the objective of creating stable suspensions to coat the structured substrates with the immersion coating technique Zeta potential and measurement of particle size are two important techniques.

Zeta potential was measured for La-Al_2O_3 and Al_2O_3 obtaining a Zeta potential curve as it is shown in the following Figure14:

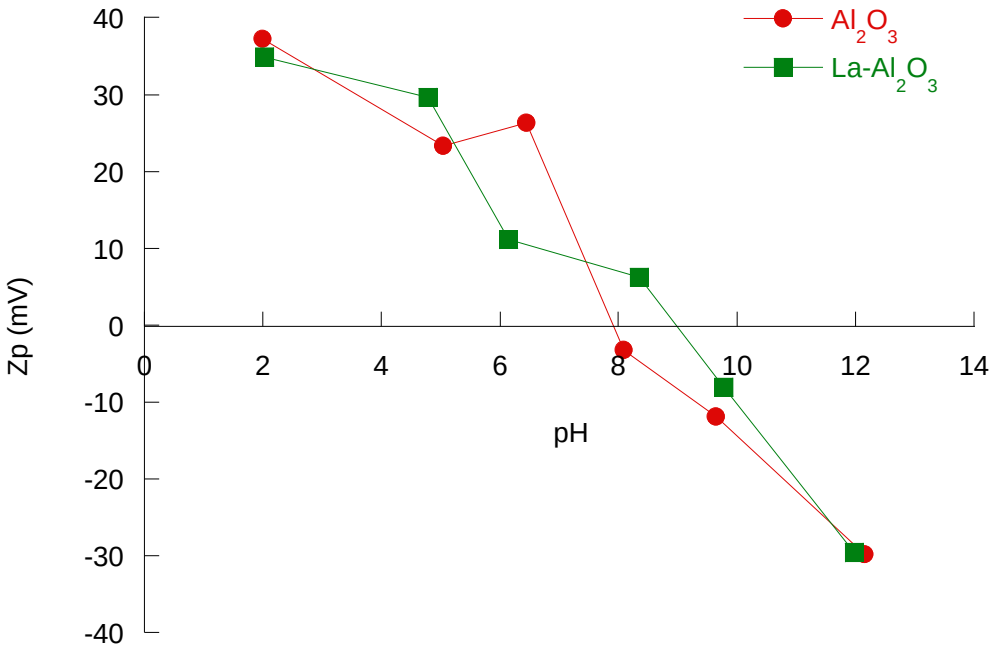

Figure 14. Zeta potential Vs pH for La-Al_2O_3 and Al_2O_3.

Figure 14 shows the adequate values of Zeta potential with the view to get stable suspensions, which are obtained in acidic pH (pH=2-4) and basic pH (pH=11-12), where the values of Zeta potential are ±30 mV. This values allow repulsion between particles,

avoiding precipitations.[46] The colloidal alumina used for the suspensions had a pH of 4, which was the reason of using a pH = 4 for the suspensions.

Particle size is another important characterization that it is indispensable to be adequate for a good suspension, for that, particle size was measured for the La-Al_2O_3 (see Figure 15). Adequate values of particle size for La-Al_2O_3 means adequate values of those derivative catalysts from the same alumina.

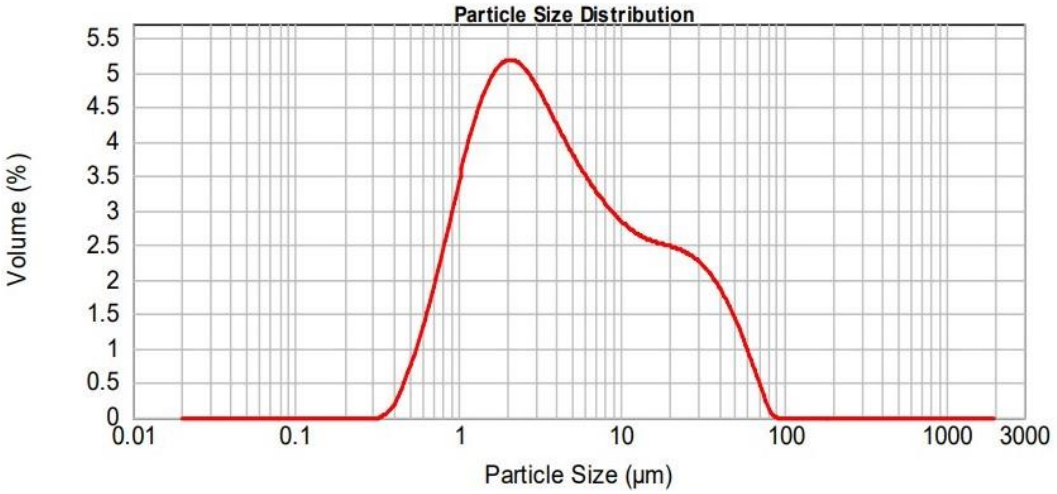

Figure 15. Distribution of particle size of the support (La-Al_2O_3).

It was stated by Agrafiotis and Cols that an adequate value of particle size to coat are those below 10 µm.[49] According to the result obtained in the measurement of particle size by laser diffraction, the particle size of the La-Al_2O_3 is adequate.

Table 5. Particle size of the prepared La-Al_2O_3.

Sample	D [4.3] (µm)
15% Ni/La-Al_2O_3	9. 602

3.2. ADDITION OF DIFFERENT PVA

In this part, knowing that the PVA makes a difference in the characterisation techniques, the properties of the added PVA will be changed. The changes will be made in the molecular weight of the polymer and also in the hydrolysis degree (see Table 2), there will be no change in the quantity added to the catalysts (Table 1). The results will be separated in the characterisation techniques used for the analysis of samples.

3.2.1. Viscosity

There are several methods to coat structured substrates: in-situ growing, sol-gel techniques, immersion coating, etc.[50] The last mentioned technique is the most used one, it consists on the introduction of the structured substrate at a controlled speed into a prepared suspension which contains the catalyst (or its precursors) and additives that stabilizes the suspension and induce the adherence of the catalyst to the outer layer of the structured substrate (Figure 16).

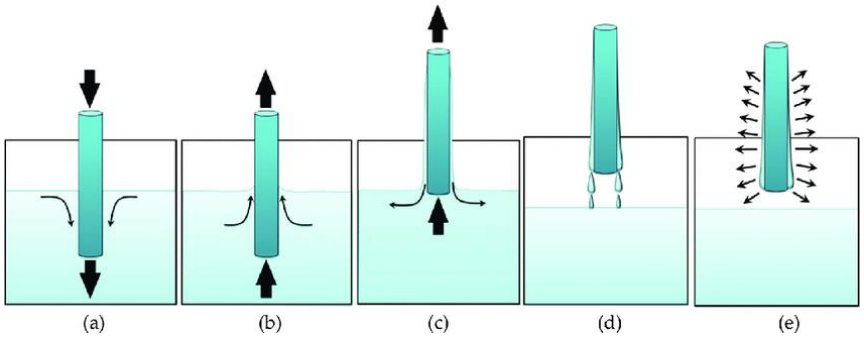

Figure 16. Coating technique via immersion.[50]

Once the structured substrate have been introduced to the suspension, it has to be maintained for a short period of time and finally it is removed from the suspension at a controlled speed. The subsequent step consists on the elimination of the excess suspension left in the canals, which is done by blowing and centrifuging.

In order to coat the structured substrates with the immersion coating technique, it is really important to obtain stable suspensions and coat the catalyst homogeneously. For that purpose, it is essential to determine adequate values of viscosity.

The viscosity was measured between 0 and 3600 s^{-1}, this values come from the coating technique, which is divided into two steps, the immersion (values between 100-1000 s^{-1}) and the centrifuging (values at 3600 s^{-1}).

Viscosity was determined for the catalysts with different PVA. Two different properties were changed, the MW and the degree of hydrolysis. Viscosity results are separated in polymers with the same hydrolysis degree but different MW (Figure 17), and polymers with variations on their hydrolysis degree (Figure 18).

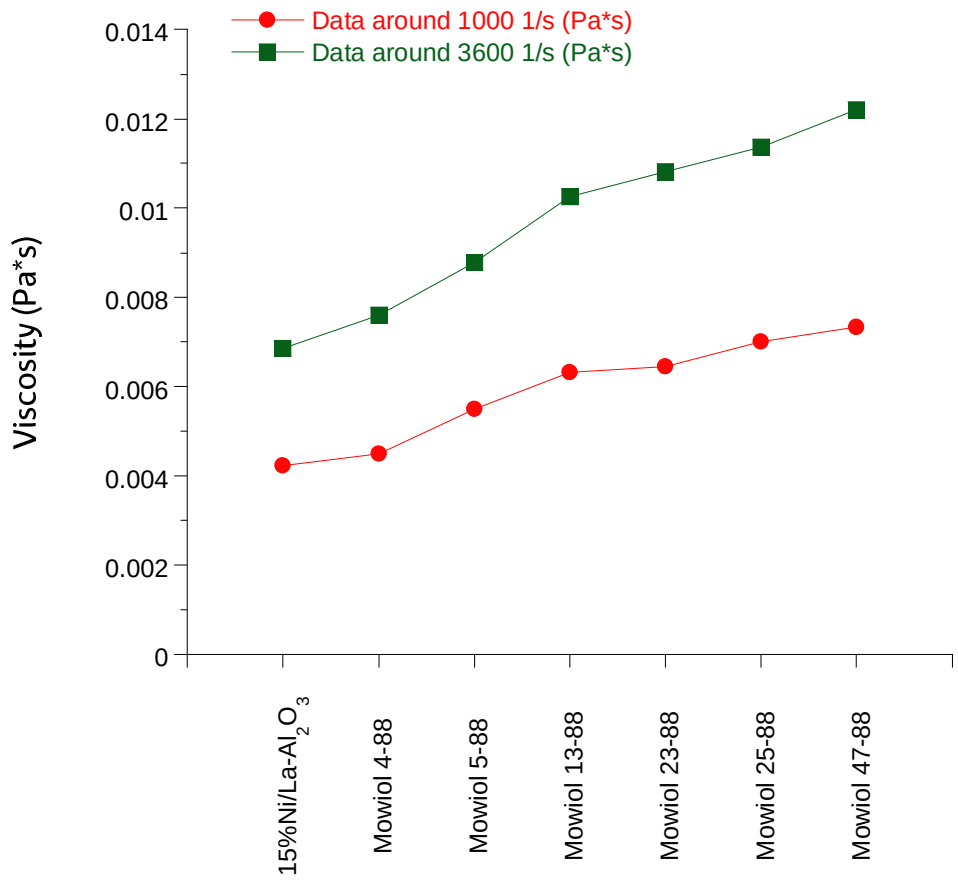

Figure 17. Viscosity measurements of slurried catalysts with different molecular weight PVA.

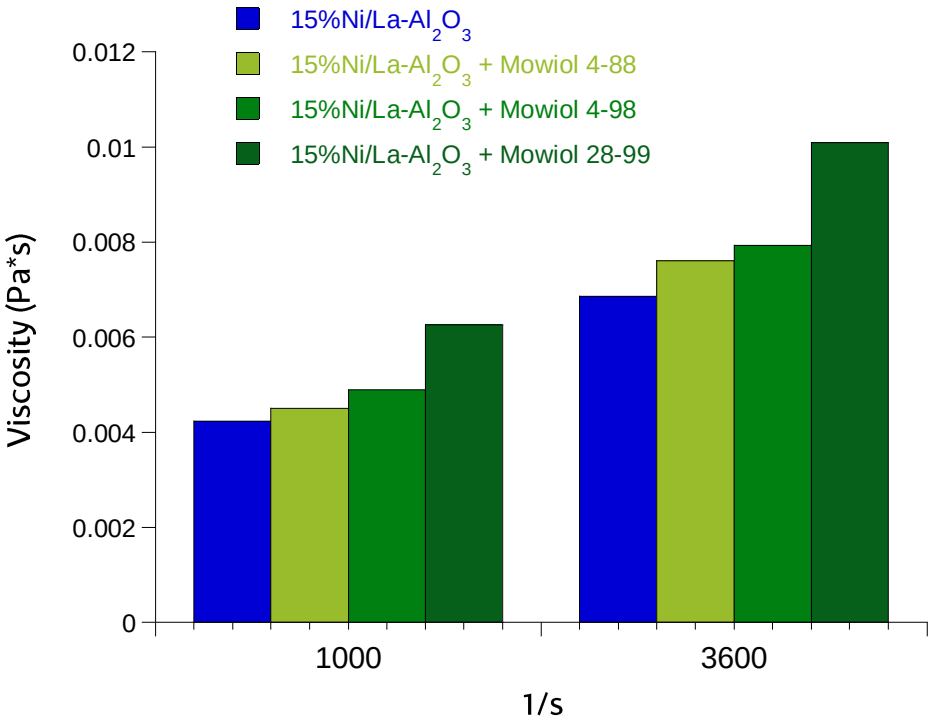

Figure 18. Viscosity measured for different hydrolysis degree Mowiols.

The results obtained in Figure 17 show that the incorporation of PVA in the catalyst suspension the viscosity increased. Moreover, the increasing on the molecular weight cause an increase on the viscosity. Specifically speaking, when the molecular weight was increased from 31,000 mol wt (PVA-Mowiol 4-88) to 138,900 mol wt (PVA-Mowiol 47-88), the value of viscosity increased from 0.004 Pa*s to 0.007 Pa*s (data around 1000 1/s) and from 0.007 Pa*s to 0.012 Pa*s (data around 3600 1/s).

According to the results obtained by measuring the viscosity with changes on the hydrolysis degree (Figure 18), even if the quantity of samples were limited (only Mowiol 4-88 and Mowiol 4-98 could be compared), it can be said that the change on the viscosity is a slight increase. However, regarding the increase in the viscosity comparing Mowiols 4-98 with 28-99, the major change seems to be given due to the growth in the molecular weight.

Samples where characterized following the steps explained in the experimental part. The values of viscosity obtained for the suspensions (0.004-0.013 Pa*s or 4-13 cP) are adequate to get stable suspensions and proper coatings.[50]

3.2.2. N_2 Physisorption: Textural properties

The textural properties of the slurried catalysts (drying and calcinating the catalysts slurries) were analysed by N_2 physisorption.

In the coming part the adsorption-desorption isotherms of N_2 (Figures 19 and 20) and the pore size distribution (Figures 21 and 22) will appear. The isotherms presented are of type IV, corresponding to mesoporous solids.

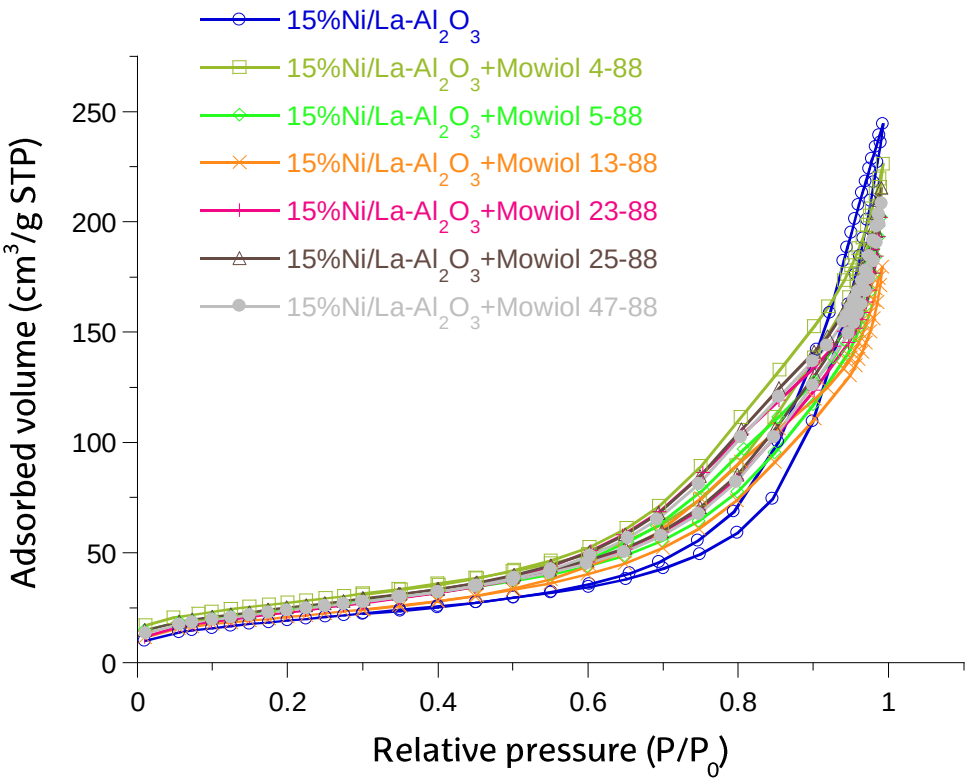

Figure 19. Adsorption-desorption isotherms of N_2, change on the MW.

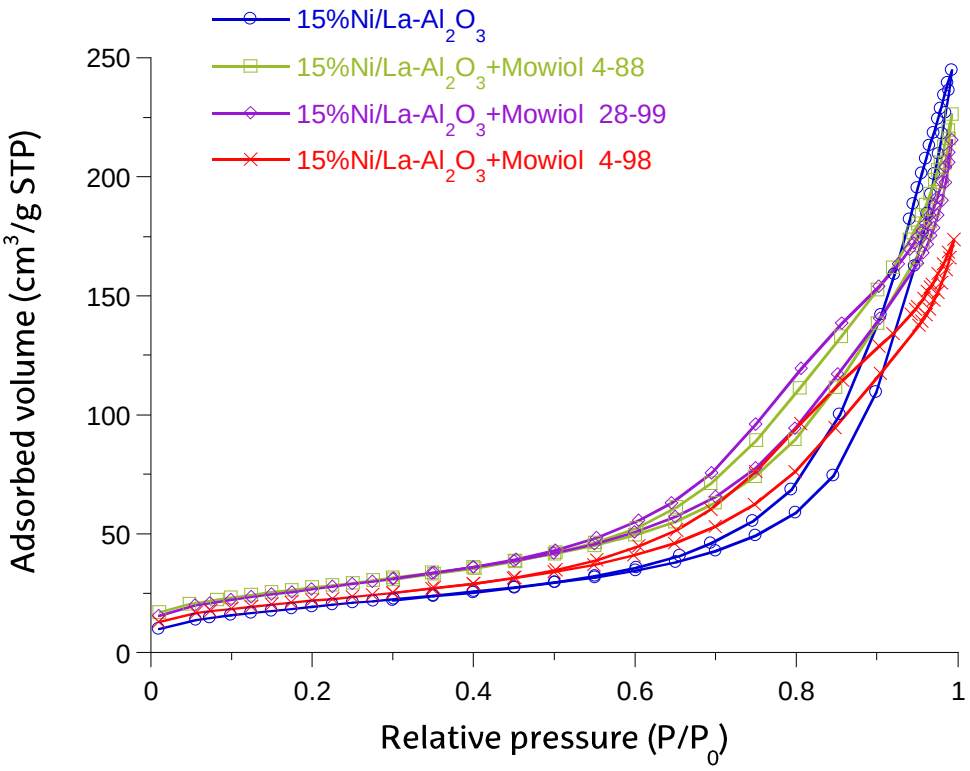

Figure 20. Adsorption-desorption isotherms of N_2, change on the hydrolysis degree.

In the case of pore size distribution (Figures 21 and 22), the main difference between catalysts with PVA and the catalyst without it, is a slight change to smaller diameter pores. The difference between almost all catalysts with PVA is mainly insignificant. Moreover, as the results obtained variate between 2-50 nm, it was verified that they are in the group of mesoporous.

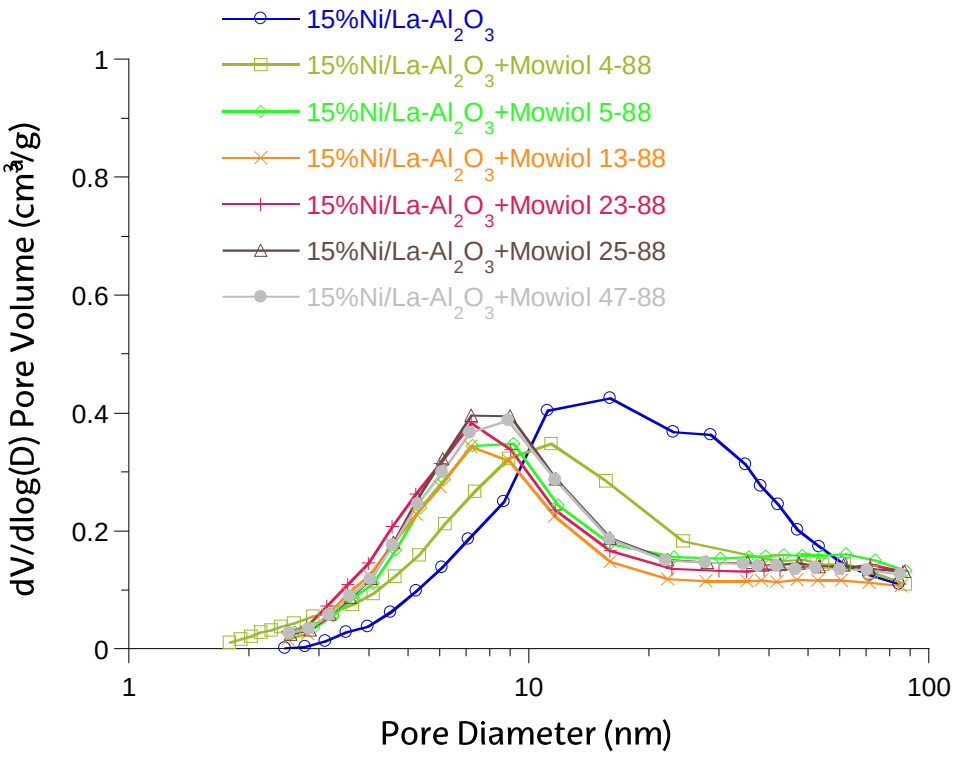

Figure 21. Pore size distribution comparison, changing MW.

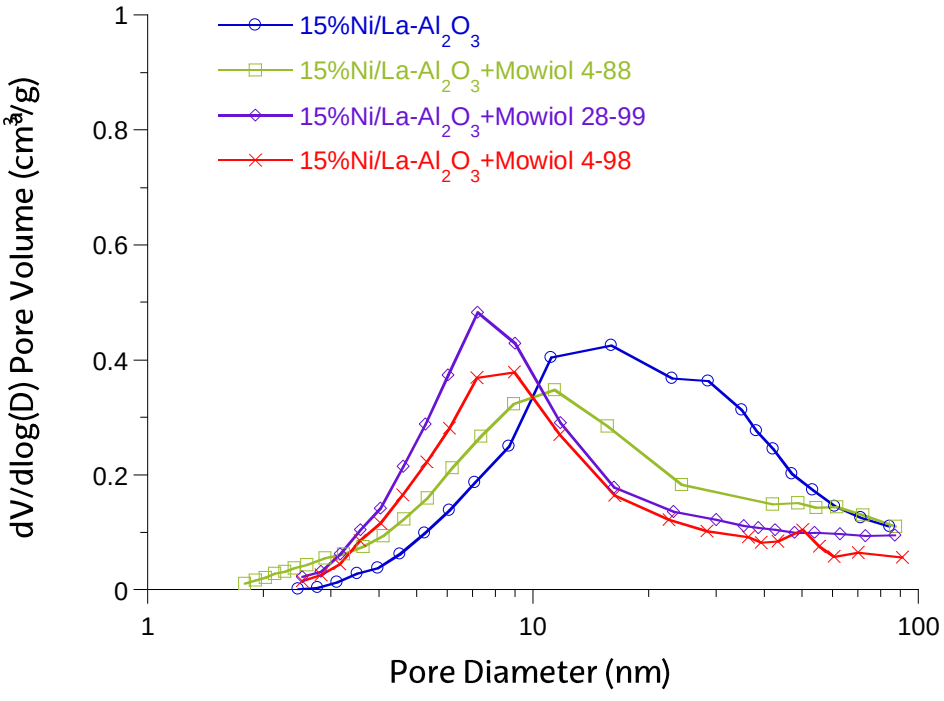

Figure 22. Pore size distribution comparison, changing the hydrolysis degree.

Table 6 shows the texture properties of the catalysts prepared with the addition of different PVA. The results between the catalysts with PVA and the catalyst without the polymer variate as an increase (almost in everyone) in the specific surface, the surface in which the active phase is disposed, and also in the pore volume, but as a decrease in the diameter of the pore.

Table 6. Texture properties of catalyst with different PVA

Sample	S_{BET} (m^2/g)	V_{pore} (cm^3/g)	D_{pore} (nm)
15% Ni/La-Al_2O_3	75.0	0.307	16.4
15% Ni/La-Al_2O_3+Mowiol 4-88	98.3	0.350	14.2
15% Ni/La-Al_2O_3+Mowiol 5-88	87.4	0.313	14.3
15% Ni/La-Al_2O_3+Mowiol 13-88	90.3	0.315	13.9
15% Ni/La-Al_2O_3+Mowiol 23-88	86.8	0.313	14.4
15% Ni/La-Al_2O_3+Mowiol 25-88	92.0	0.333	14.5
15% Ni/La-Al_2O_3+Mowiol 47-88	88.2	0.322	14.6
15% Ni/La-Al_2O_3+Mowiol 28-99	98.1	0.333	13.6
15% Ni/La-Al_2O_3+Mowiol 4-98	79.0	0.269	13.6

3.2.3. Chemical adsorption of the catalysts

The results obtained from the chemical adsorption of CO are presented in the following part. The Table 7 shows every significant result obtained for the slurried catalysts with PVA in their formulation, all of them prepared with the "All in one" method.

The dispersion and particle size ($D_{p\ (Ni^0)}$) are inversely proportional, when the particle size of the nickel decreases the dispersion increases. The reducibility is the

quantity of NiO that reduces (%), the largest particles have a higher reduction capability and the metallic surface has to be as large as possible in order to have as much active surface for the Sabatier reaction.

With the addition of PVA, the changes are given in the dispersion and in the metallic surface (cat. and metal), increasing their values until Mowiol 25-88, which gives a decrease in the dispersion and an increase in the particle size. Nevertheless, there is a decrease in both, the particle size and the reducibility.

Moreover, comparing the catalysts with variations in the hydrolysis degree (Mowiol 4-98 and 28-99) slight differences were obtained.

Table 7. Chemical adsorption of CO and oxidation of O_2, samples with the addition of PVA.

Sample	Dispersion (%)	$D_{p\,(Ni^0)}$ (nm)	Reducibility (%)	Metallic surface (m^2/g Cat.)	Metallic surface (m^2/g metal)
15% Ni/La-Al_2O_3	14.8	5.5	80.6	14.7	98.2
15% Ni/La-Al_2O_3+Mowiol 4-88	20.9	3.3	72.6	20.9	139.2
15% Ni/La-Al_2O_3+Mowiol 5-88	23.3	3.2	73.6	23.3	155.0
15% Ni/La-Al_2O_3+Mowiol 13-88	29.0	2.7	77.7	29.0	193.3
15% Ni/La-Al_2O_3+Mowiol 23-88	28.7	2.7	76.0	28.7	191.1
15% Ni/La-Al_2O_3+Mowiol 25-88	20.0	3.9	77.1	20.0	133.1
15% Ni/La-Al_2O_3+Mowiol 47-88	22.0	3.4	74.5	22.0	146.7
15% Ni/La-Al_2O_3+Mowiol 28-99	26.3	2.8	74.0	26.3	175.1
15% Ni/La-Al_2O_3+Mowiol 4-98	24.3	3.1	75.5	24.3	162.1

3.2.4. X-ray diffraction

The structured properties of the catalysts were characterised by the X-ray diffraction technique. In each diffractogram (Figures 23 and 24) it can be seen that the principle species are α-Al_2O_3 (JCPDS 00-029-0063), NiO (JCPDS 01-073-1519) and nickel spinel ($NiAl_2O_3$) (JCPDS 00-010-0339). The fundamental positions for α-Al_2O_3 are 2θ = 19.85º, 31.94º, 37.6º, 45.79º and 60.45º. In case of NiO, the principal position are 2θ = 37.33º, 43.38º and 63.02º. Finally, the peaks corresponding to $NiAl_2O_3$ appear in the positions 2θ = 19.07º, 31.41º, 45º, 65.54º, 69º, and 77.74º.

In Figure 23 it can be observed that the addition of the PVA affects directly to those peaks corresponding to the NiO, decreasing the intensity and obtaining a broader peaks. However, the rest of the peaks, the ones that belong to the species Al_2O_3 and $NiAl_2O_3$ spinel, do not suffer a noticeable change. Furthermore, comparing the hydrolysis degree (Figure 24), the results do not seem to variate when increasing the hydrolysis degree but more samples would be necessary to confirm that.

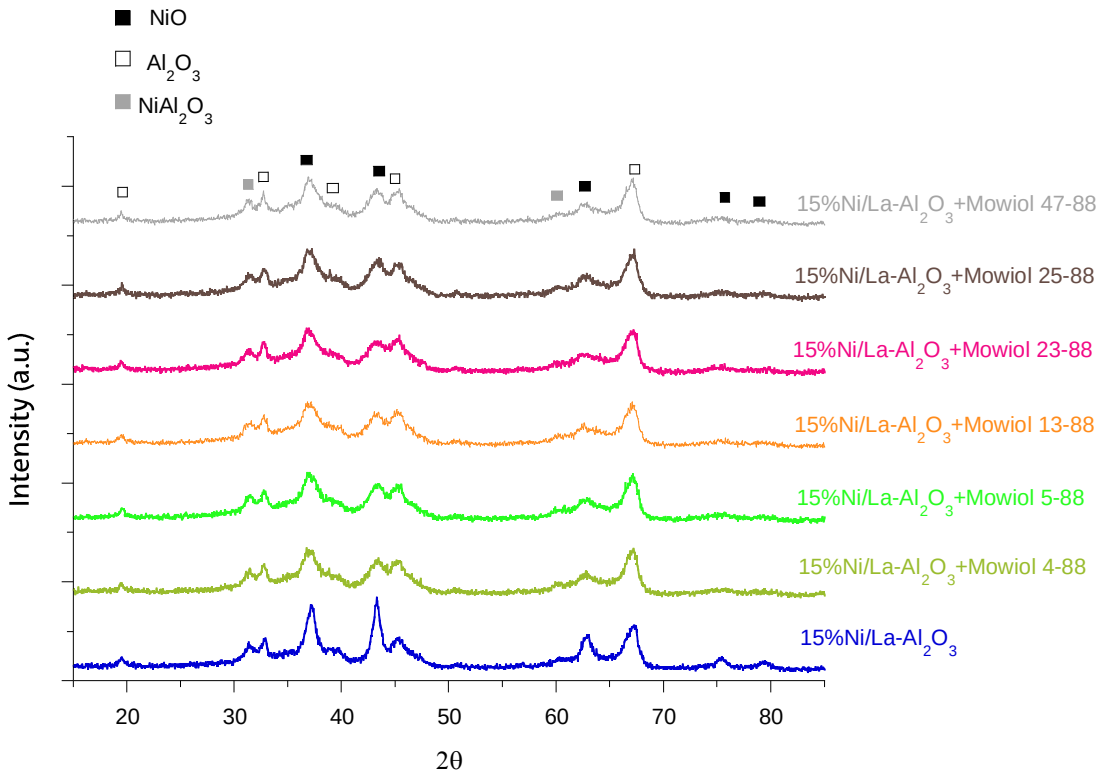

Figure 23. X-ray diffraction for catalysts with PVA, change of the MW.

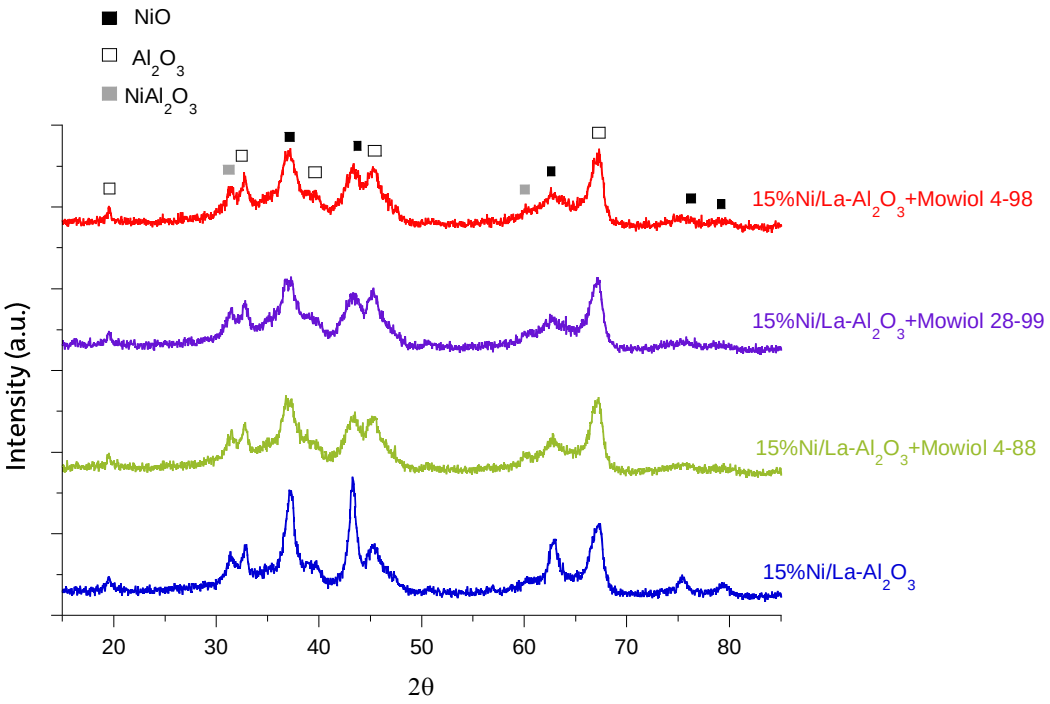

Figure 24. X-ray diffraction for catalysts with PVA, change of the hydrolysis degree.

Particle size of nickel was also measured by XRD applying Scherrer's equation (see experimental part), and it can be seen in the results obtained (Table 8) where the size decreases with the addition of the PVA. Furthermore, an increase on the MW decreases the particle size and hydrolysis degree has the same effect.

Table 8. Different PVA, XRD particle size results.

Sample	Size of the Ni^0 (nm)		Sample	Size of the Ni^0 (nm)
15% Ni/La-Al_2O_3	10.04		15% Ni/La-Al_2O_3+ Mowiol 4-88	7.44
15% Ni/La-Al_2O_3+ Mowiol 5-88	6.25		15% Ni/La-Al_2O_3+ Mowiol 13-88	5.87
15% Ni/La-Al_2O_3+ Mowiol 23-88	6.02		15% Ni/La-Al_2O_3+ Mowiol 25-88	6.14
15% Ni/La-Al_2O_3+ Mowiol 47-88	3.48		15% Ni/La-Al_2O_3+ Mowiol 28-99	6.00
15% Ni/La-Al_2O_3+ Mowiol 4-98	5.87		-	-

3.2.5. TPR

Temperature programmed reduction was used for those catalysts with the best results from other characterisation techniques, regarding the nickel particles size and the dispersion, the importance of those factors are explained in the introduction (Sabatier reaction).

With this technique the number and the type of reductive species in the catalysts will be analysed in order to obtain information about the interaction between the active phase and the support. TPR was used to determine the reducibility of the catalysts up to 1000 ºC, where the species of nickel oxide use to be divided in three different parts (Figure 25, α, β and γ).

The peaks appearing at low temperature regime (300-450 ºC) belong to the α-NiO type species, concerning weak interactions between the support and the NiO free species. At medium temperatures (450-700 ºC), the species β-NiO are found, which presents a higher interaction between the support than the α-NiO type species. Finally, the peaks at high temperatures (700-1000 ºC) correspond to γ-NiO. This type of nickel oxides show a highly stable nickel aluminate phase with a spinel structure, which are very difficult to reduce, so smaller peaks means better results.

In the following Figure 25 the results obtained from the temperature programmed reduction for the selected catalysts are shown. As it can be appreciated, the addition of PVA (Mowiol 4-88) causes a decrease on the reduction temperature of the species α-NiO and species β-NiO. Also, increasing the molecular weight of the added polymer, the reduction temperature suffers even more decrease. With this data it can be said that the reducibility increases with the addition of PVA and also with the increasing of the molecular weight in two species, α-NiO and β-NiO

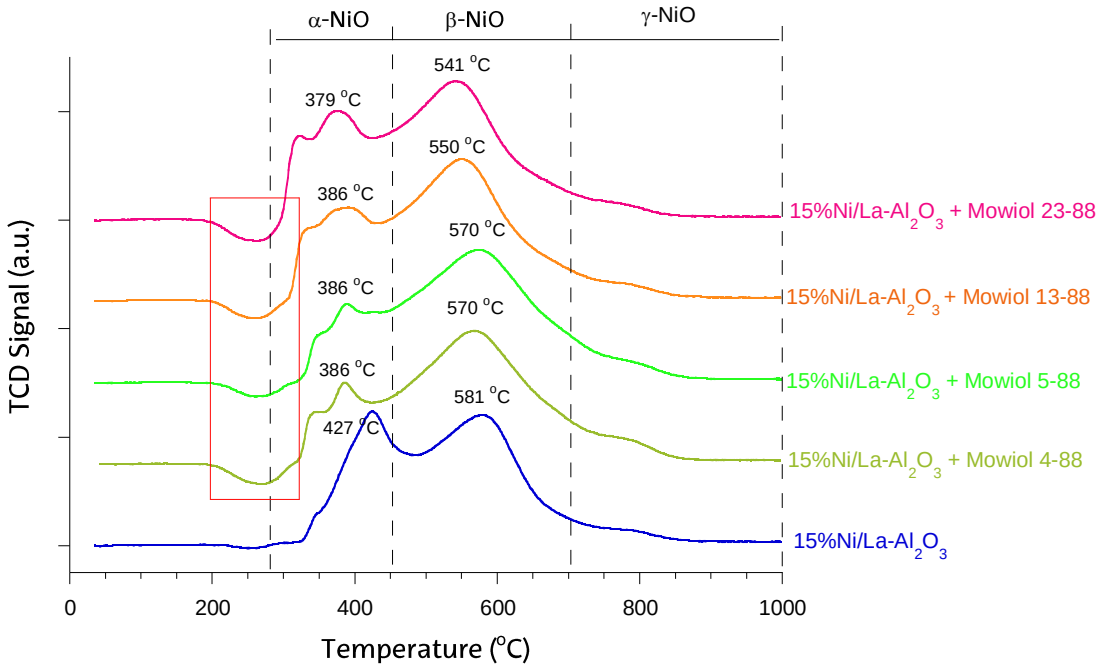

Figure 25. TPR of the selected catalysts.

In the Table 9 the values obtained from the TPR technique for the selected catalysts are shown. It can be appreciated that the reducibility until 1000 °C gives values a little bit higher than 100%, this could be because the quantity of Ni in the catalysts (15%) is higher than the theoretical one.

Figure 9. Theoretical and experimental consumption of H_2 for the selected catalysts.

Sample	H_2 consumed (g)		Reducibility
	Theoretical	Experimental	(%R)
15% Ni/La-Al_2O_3	0.00065	0.00073	112.0
15% Ni/La-Al_2O_3 + Mowiol 4-88	0.00066	0.0007	106.4
15% Ni/La-Al_2O_3 + Mowiol 5-88	0.00065	0.00072	111.9
15% Ni/La-Al_2O_3 + Mowiol 13-88	0.00066	0.00074	112.8
15% Ni/La-Al_2O_3 + Mowiol 23-88	0.00064	0.00075	118.1

3.3. ADDITION OF PVP

In this part the results from the characterisation techniques made for those catalysts prepared with the addition of PVP will appear. There were used different variations of PVP altering the MW. The formulation used for the preparation was the same for every polymer added always using the "All in one" method, the results will be separated by characterisation technique.

3.3.1. Viscosity

Viscosity was measured to compare the changes suffered when PVP was added, the values of viscosity obtained for the suspensions have to be between 0.004-0.013 Pa*s (4-13 cP), in this scale the values will be adequate to get stable suspensions and proper coatings[49] (Figure 26).

Values of viscosity increase with higher MW, in data around 1000 1/s the value of viscosity increases from 0.004 Pa*s (MW = 10,000 mol wt) to 0.007 Pa*s (MW = 360,000 mol wt) and corresponding to data around 3600 1/s the increase is given from 0.007 Pa*s to 0.011 Pa*s.

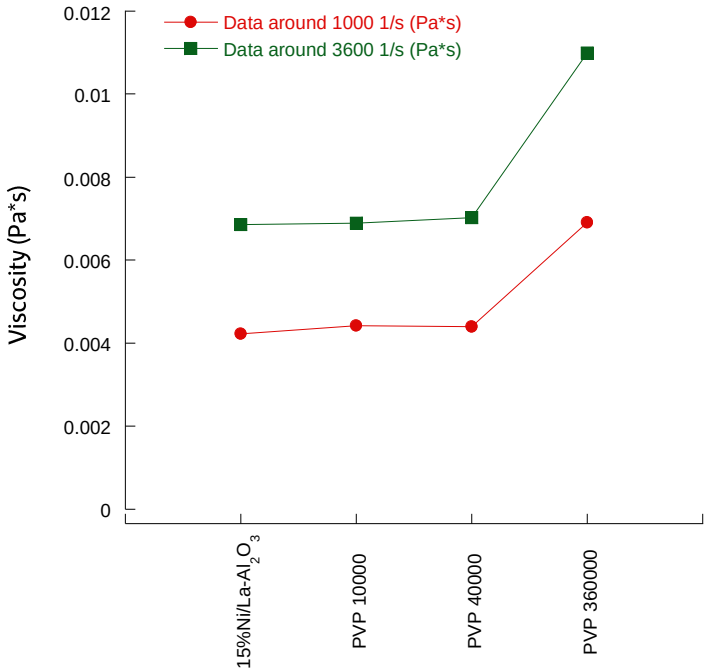

Figure 26. Viscosity of suspensions prepared with different MW PVPs.

3.3.2. N_2 Physisorption: Textural Properties

In the upcoming Figures 27 and 28, adsorption-desorption isotherm and pore size distribution will be shown to compare the catalysts prepared with PVP in the formulation, isotherms are of type IV, corresponding to mesoporous solids. The results obtained variate with the same behaviour observed incorporating PVA (Figure 19 and 21).

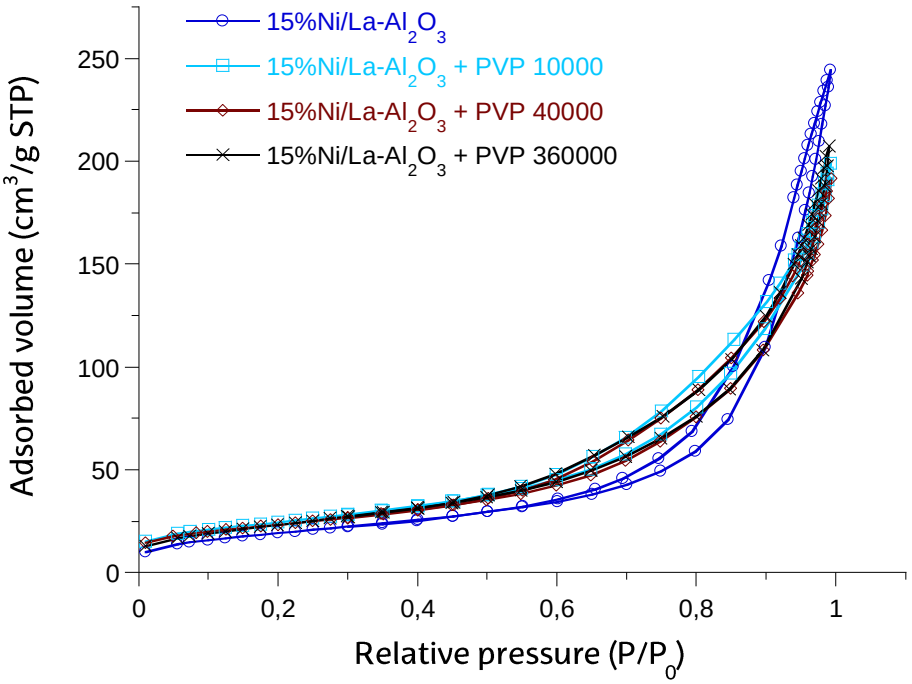

Figure 27. Adsorption-desorption isotherms. Addition of PVP.

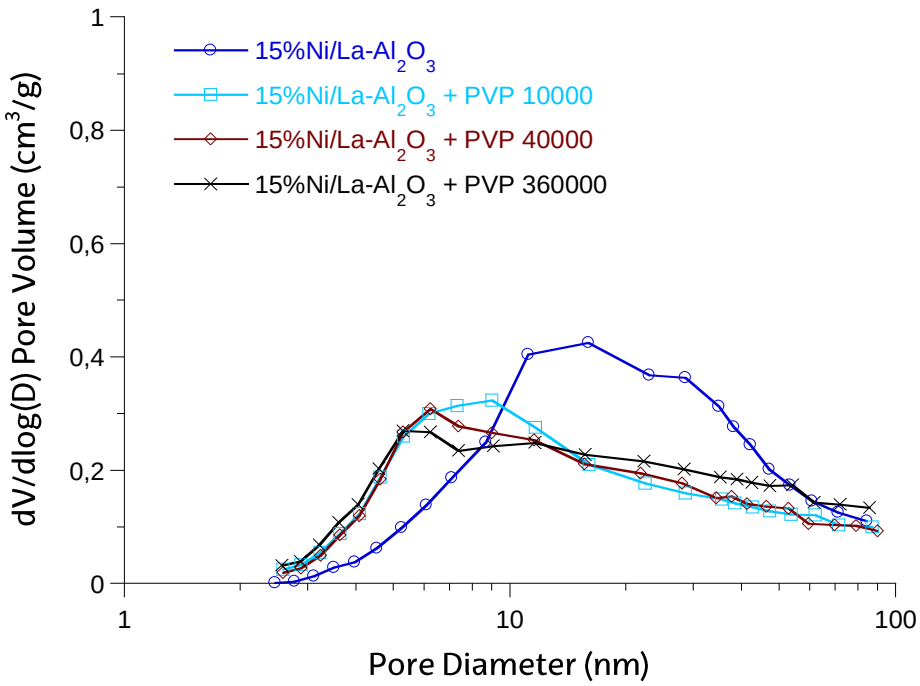

Figure 28. Pore size distribution. Addition of PVP.

The table below (Table 10) shows the results for the texture properties obtained when analysing the catalysts with PVP. In comparison with the reference catalyst (15% Ni/La-Al_2O_3), the results variate the same way as with PVA, S_{BET} and pore volume increase while the pore diameter decrease. In this case a pattern is followed: increasing the molecular weight cause a decrease in the pore diameter.

Table 10. Texture properties by N_2 physisorption with the addition of PVP.

Sample	S_{BET} (m^2/g)	V_{pore} (cm^3/g)	D_{pore} (nm)
15% Ni/La-Al_2O_3	75.0	0.307	16.4
15% Ni/La-Al_2O_3+PVP 10000	88.8	0.308	13.9
15% Ni/La-Al_2O_3+PVP 40000	83.6	0.31	14.2
15% Ni/La-Al_2O_3+PVP 360000	86.9	0.321	14.8

3.3.3. Chemical adsorption

As with PVA, the catalysts prepared with the addition of PVPs were characterized using the chemical adsorption technique. The following results are those obtained from the mentioned technique for the three catalyst with PVP in their formulation and the catalyst without polymer.

According to these results, the dispersion of nickel with the addition of PVP increases, but the differences between the distinct MW is almost unnoticeable. Same happens with almost every result obtained, they increase or decrease in comparison with 15% Ni/La-Al_2O_3, always improving the value of the corresponding result, but there are minor differences between those with PVPs. The results obtained are presented in the following Table 11.

Table 11. Chemical adsorption of CO and oxidation of O_2, catalysts with PVP.

Sample	Dispersion (%)	$D_{p\,(Ni^0)}$ (nm)	Reducibility (%)	Metallic surface (m^2/g Cat.)	Metallic surface (m^2/g metal)
15% Ni/La-Al_2O_3	14.7	5.5	80.6	14.7	98.2
15% Ni/La-Al_2O_3+PVP 10000	18.7	4.0	73.8	18.7	124.8
15% Ni/La-Al_2O_3+PVP 40000	17.4	4.4	75.5	17.3	115.5
15% Ni/La-Al_2O_3+PVP 360000	19.0	4.0	74.4	18.9	126.3

3.3.4. X-ray diffraction

Once more, the structured properties of the catalysts has to be determined using the X-ray diffraction technique (Figure 29). The signals of the diffractogram corresponding to those of the NiO are less intense with the addition of PVP. However, the rest of the signals, the ones of Al_2O_3 and $NiAl_2O_3$, seems to have no change even when adding the polymer.

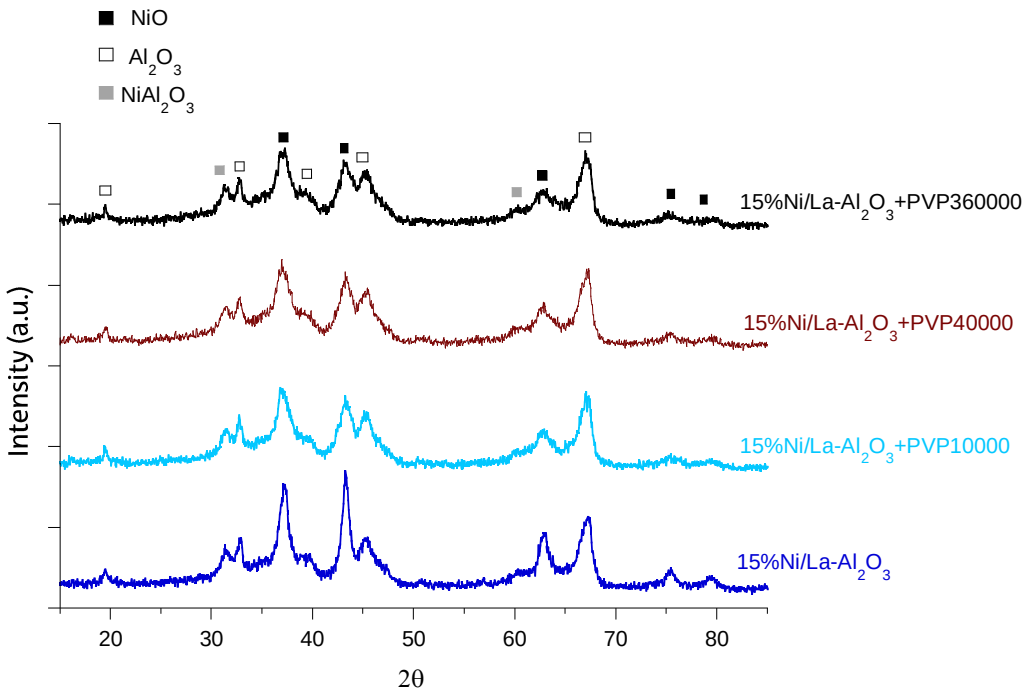

Figure 29. X-ray diffraction for the catalysts prepared with PVP.

One the other hand, the results for the Ni^0 crystal size obtained from the X-ray diffraction technique (Table 12), can be appreciated the slight decrease that occurs when increasing the molecular weight of the added PVP. Furthermore, the crystal size decreases from the catalyst without polymer to those who have it.

Table 12. Ni^0 crystal size with the addition of PVP.

Sample	Size of the N^0 (nm)
15% Ni/La-Al_2O_3	10.04
15% Ni/La-Al_2O_3 + PVP 10000	6.54
15% Ni/La-Al_2O_3 + PVP 40000	6.48
15% Ni/La-Al_2O_3 + PVP 360000	6.34

3.4. ADDITION OF PEG

The following part will show the results obtained for those catalysts prepared with PEG, the characterization techniques will be the same used for all the previous catalysts. Two different PEG were added, PEG 2000 and PEG 3350, they will be compared with 15% Ni/La-Al_2O_3, the catalyst without polymer.

3.4.1. Viscosity

To measure the viscosity and confirm that the suspensions prepared are adequate for coating techniques, the procedure explained in the experimental part (part 2.2.1. viscosity) was used. As it can be seen in Figure 30, the addition of the PEG increases the viscosity of the prepared suspension. Even so, the values of the viscosity for both suspensions are adequate for coating techniques (between 0.004 and 0.013 Pa*s).

With the addition of this polymer, as the molecular weights were very close, the values of viscosity had slight changes compared with the ones obtained with the addition of PVA or PVP. The viscosity changes from 0.004 Pa*s (MW = 2000 mol wt) to 0.005 Pa*s (MW =3350 mol wt) in data around 1000 1/s, and increases from 0.0065 to 0.007 in data around 3600 1/s.

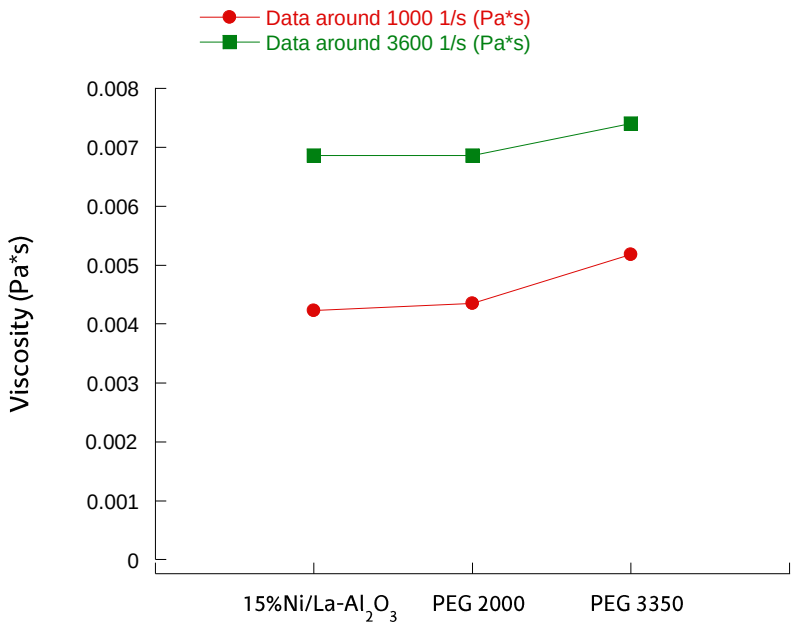

Figure 30. Viscosity measured for catalysts with PEG.

3.4.2. N_2 Physisorption: Textural Properties

The N_2 physical adsorption technique was used to ascertain the texture properties of the catalysts. Adsorption-desorption and pore size distribution isotherms of type IV (mesoporous solids) will be shown in the following Figures 31 and 32, comparing both catalysts prepared with PEG on its formulation (PEG 2000 and 3350) with the non-polymer catalyst. The adsorption-desorption isotherm and pore size distribution shows the same behaviour obtained for PVA and PVP (Figures of PVA 19-21 and Figures of PVP 27-28).

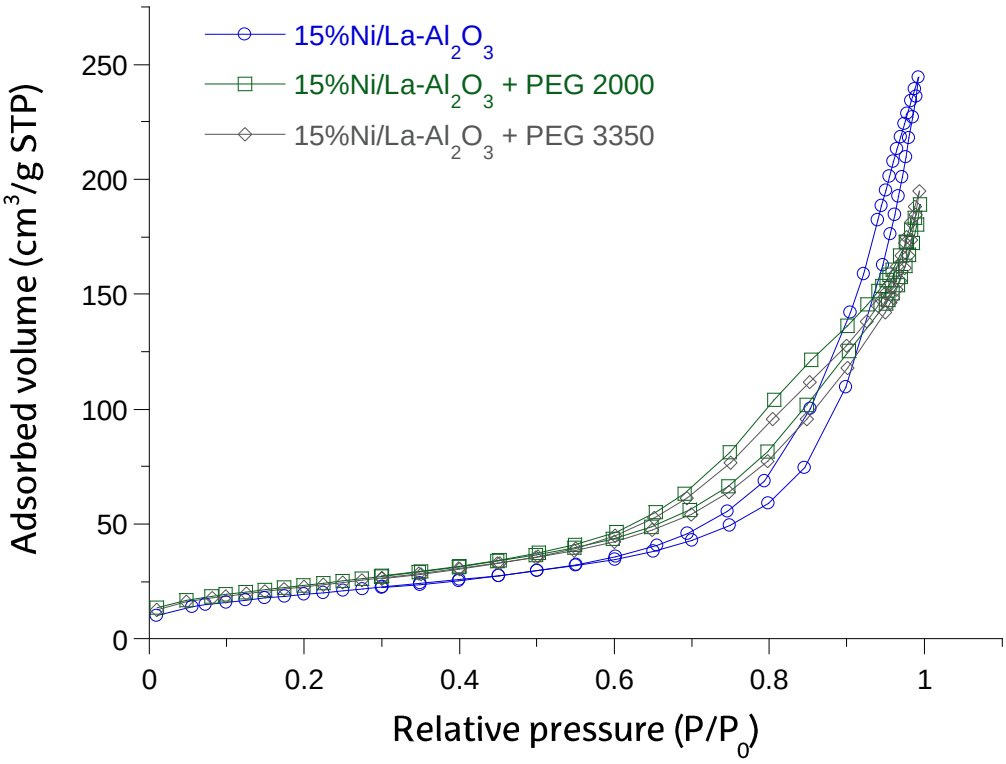

Figure 31. Adsorption-desorption isotherms of the catalysts with PEG.

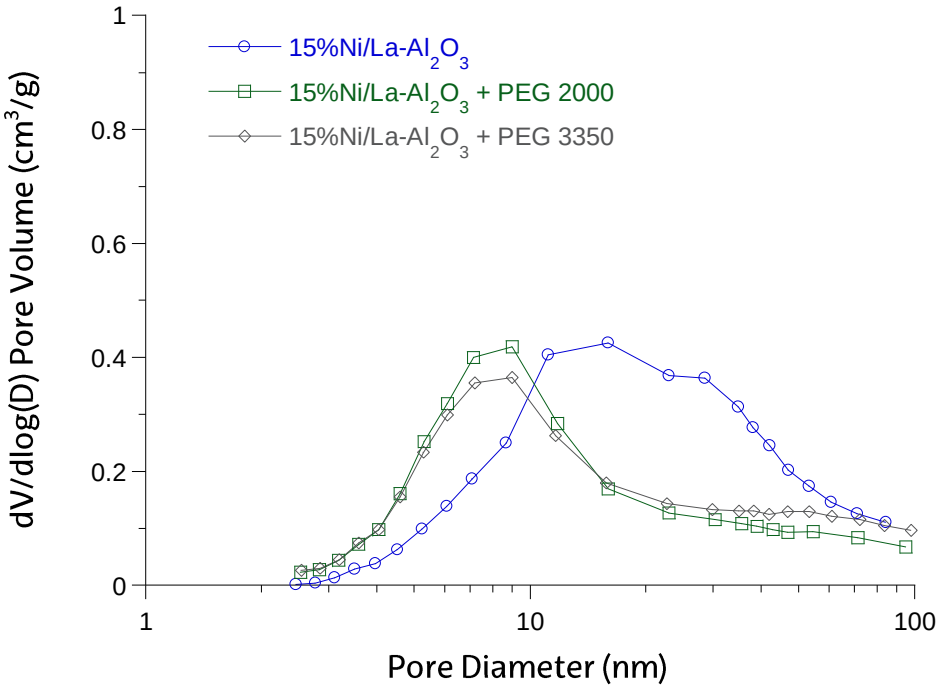

Figure 32. Pore size distribution of catalysts with PEG.

Table 13 presents the texture properties obtained in this characterization technique, comparing the ones acquired for the catalysts with PEG with the reference catalyst (15% Ni/La-Al_2O_3). The BET surface area increases with both polymers and the volume and width of the pore decreases.

Table 13. Texture properties for catalysts with PEG.

Sample	S_{BET} (m^2/g)	V_{pore} (cm^3/g)	D_{pore} (nm)
15% Ni/La-Al_2O_3	75.0	0.307	16.4
15% Ni/La-Al_2O_3+PEG 2000	85.8	0.292	13.6
15% Ni/La-Al_2O_3+PEG 3350	84.2	0.301	14.3

3.4.3. Chemical adsorption

Catalysts prepared with the addition of PEG in the formulation were also characterized using chemical adsorption technique. In the following Table 14 the results obtained from this technique will be shown.

As it can be seen the addition of a higher molecular weight PEG causes an increase on the dispersion and both metallic surfaces. However, the nickel diameter remains more or less constant even if the MW is higher, but decreases with respect to 15% Ni/La-Al_2O_3.

Table 14. Results from chemical adsorption.

Sample	Dispersion (%)	$D_{p\,(Ni^0)}$ (nm)	Reducibility (%)	Metallic surface (m^2/g Cat.)	Metallic surface (m^2/g metal)
15% Ni/La-Al_2O_3	14.8	5.5	80.6	14.7	98.2
15% Ni/La-Al_2O_3+PEG 2000	21.8	3.5	75.9	21.8	145.2
15% Ni/La-Al_2O_3+PEG 3350	25.2	3.2	78.4	25.2	167.7

3.4.4. X-ray diffraction

In the following Figure 33 the diffractogram for slurried catalysts prepared with the "All in one" method will appear. In this case, the intensity of the peaks referring to the specie NiO decreases but those that correspond to Al_2O_3 and $NiAl_2O_3$ does not seem to have any change.

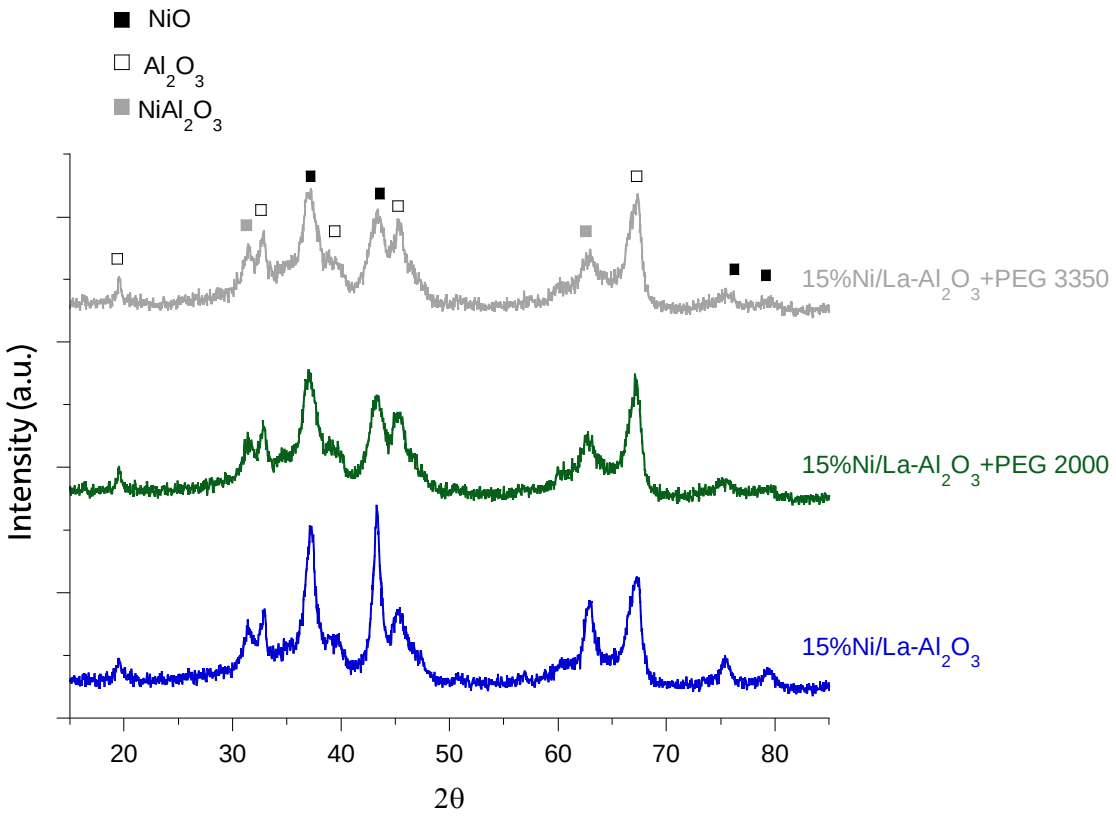

Figure 33. Diffractogram of catalysts with PEG.

Regarding to the nickel particle size by means of XRD (Table 15), it can be appreciated that the nickel size decreases when adding a PEG. In reference to the results obtained with the variation of the MW, the size of the nickel have a slight change, almost insignificant.

Table 15. Crystal size of Ni^0 of samples with PEG.

Sample	Size of the N^0 (nm)
15% $Ni/La\text{-}Al_2O_3$	10.04
15% $Ni/La\text{-}Al_2O_3$ + PEG 2000	6.2
15% $Ni/La\text{-}Al_2O_3$ + PEG 3350	6.4

4. DISCUSSION

The objective of this work is to examine the structuration of the catalysts Ni/La-Al_2O_3 to improve the Sabatier reaction when adding a polymer into their formulation. For that three different polymers have been used, PVA, PVP and PEG, varying the molecular weight of the three polymers and in case of PVA, also the hydrolysis degree.

4.1. EFFECT OF THE MOLECULAR WEIGHT IN THE VISCOSITY

The molecular weight affects directly to the viscosity of the prepared suspensions, the increasing of the first mentioned parameter increases the viscosity, and the decreases of it causes a decrease on the viscosity as it can be seen on the Figures 17, 18, 26 and 30.

The reason of this can be explained with the "reptation model" (Figure 34), a model described by Pierre-Gilles de Gennes that explains the thermal motion of long polymer chains within a tube, where the tube represents the topological constraints imposed by entanglements with other chains.[52] Inside the tube, increasing the molecular weight will cause a growth in the length of the chains, which will result in an increase of the entanglements between chains, making the suspension more viscous.

On the other hand, a decreasing on the molecular weight will cause, in simple words, an easier moving of the polymer chains within the tube, which will give a decreasing on the viscosity of the suspension.[51]

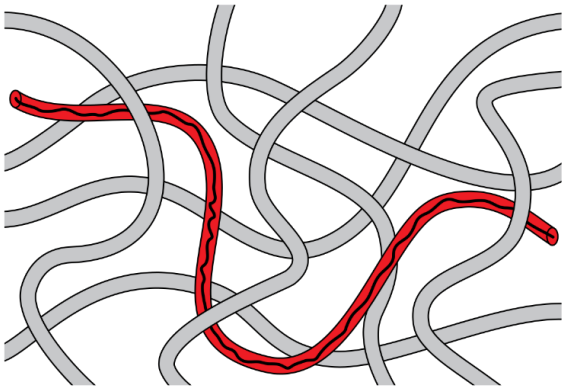

Figure 34. Reptation model of polymer chains.[52]

4.2. EFFECTS OF THE ADDITION OF PVA INTO THE FORMULATION OF CATALYSTS

The catalysts were prepared with the "All in one" method, which allows in one single step prepare a catalytic suspension for the coating of structured substrates. For that, the suspension must include apart from the alumina (the support), the water and the active phase: Ni, additives that stabilizes the suspension and induce the adhesion of the catalysts to the structured substrates. However, making use of these additives can cause modifications in the catalytical properties of the catalyst.[6, 53, 54]

In this part the effect of the PVA added to the suspensions has been studied, taking into account that were used PVAs with different MW and hydrolysis degrees.

With the chemical adsorption technique the dispersion and nickel particle size obtained with the different catalysts has been determined. As it can be seen in Table 7 the increasing of the molecular weight causes an increase in the dispersion and a decrease in the particle size up to a critical MW (92,600 mol wt, Mowiol 25-88). In chemical adsorption from the critical molecular weight forward, the particle size increases. This could be the result of an inadequate calcinating temperature, due to the fact that this temperature increases with the molecular weight, giving as a result, an amount of polymer (PVA) without removing, surrounding the nickel particle and causing interferences on the adsorption of CO.[55] However, using XRD (Table 8), the nickel particle size decreases with the increasing of the MW, which confirms that the Ni particle size evolves inversely to the molecular weight.

To obtain reliable information about the cause of that increasing in the particle size from the critical MW forwards, calcinating temperature used for those catalysts could be increased, as well as using a thermogravimetric analysis technique to get the needed data.

Nevertheless, taking into account the results obtained from the previously mentioned characterization techniques, it can be said that the addition of PVA into the formulation of the catalysts suspensions makes a difference into the dispersion and particle size. As it is shown in Figure 35, with a higher MW polymer, the distance and repulsion between the nickel particles is higher, avoiding aggregation. However, with smaller molecular weight polymers, the Ni particles are closer.

Moreover, the increasing of the molecular weight of the polymer also affects both factors, dispersion and particle size, increasing the first one and decreasing the last one.

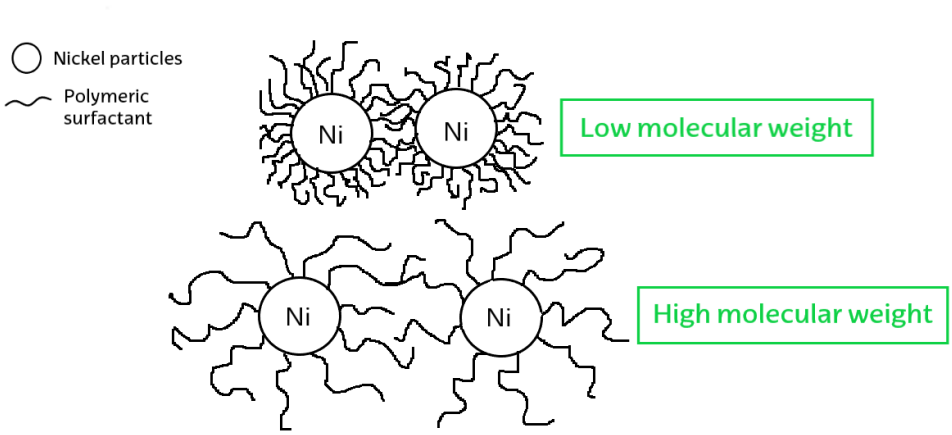

Figure 35. The effect MW does on the dispersion of the particles

Additionally, the hydrolysis degree was also variated. Increasing it appears to have the same effect molecular weight has on the dispersion and the particle size, but at lower levels (Table 7), increasing one and decreasing the last. Nonetheless, with the amount of catalysts prepared with a variation on the hydrolysis degree we cannot assure this fact. To get trustworthy information about how the hydrolysis degree affects the catalysts we would need to prepare and test more samples.

4.3. EFFECTS OF THE ADDITION OF PVP AND PEG INTO THE FORMULATION OF THE CATALYSTS

In this part the effects caused by the addition of two different polymers will be exposed taking into account the variation on the molecular weight for both polymers.

Looking at the results obtained from both XRD analysis (Tables 12 and 15), it can be seen that the particle size of the nickel is not varying with the variation of the molecular weight for both polymers, in contrast with the particle sizes obtained with the addition of PVA, which suffers a notorious decrease when the MW increased. This fact can be confirmed also by looking at the results obtained in chemical adsorption (Tables 11 and 14), which confirms that with PVP or PEG, even with variation in their MW, particle size remains constant.

In reference to the values of the dispersion for the catalysts with PVP or PEG on their formulation, the dispersion only increases with higher molecular weights of PEG, and suffers no variation when increasing the one of the PVP (Tables 11 and 14). Michaella Signoretto wrote an article about the effects support and synthetic procedure for sol-immobilized Au nanoparticles is shown, which obtained results similar to ours, getting worst performance with the samples prepared by colloidal method with PVP.[55]

To summarize, the particle size for both PVP and PEG remains constant even if the molecular weight of them increases, that is why we can assume that the increasing of the molecular weight has no effect on the particle size (Tables 12 and 15). Moreover, the dispersion in case of adding PVP, even if the MW is increased, will not vary, being not dependant on the MW (Table 11). However, the dispersion with PEG seems to increase with the molecular weight (Table 14).

In order to obtain firm information we would need to characterize with all the techniques previously mentioned a larger quantity of catalysts with PVP and PEG, varying the molecular weight of both polymers. What is more, the information about these polymers is so reduced it is almost impossible to find information about them for techniques similar to the ones made in our laboratory group.

4.4. COMPARISON BETWEEN POLYMERS

In the following part the results obtained from each polymer will be compared in order to determine the best polymer to use into the formulation of catalysts for the Sabatier's reaction.

From the characterisation techniques the nickel particle size and the dispersion were calculated, both aspects really significant with the view of catalysing. The chemical adsorption and XRD give values of particle sizes and as it can be seen in Tables 8, 12 and 15 (nickel sizes by XRD), the best results were obtained with the PVA, specifically with the highest molecular weight PVA (Mowiol 47-88). In spite of this, the particle sizes obtained for the catalysts with the addition of PVP and PEG were almost equal, decreasing their values compared with the catalyst without polymer.

On the other hand, the dispersion was acquired by chemical adsorption, from which the best results were obtained with the PVA (Table 7), improving the dispersion

from the catalyst without polymer to a maximum of a 14%. According to PEG and PVP (Tables 11 and 14), even if with both polymers the dispersion is increased, the molecular weight in case of PVP does not seem to have any impact on it, however, the MW in PEG appears to have some effect on the dispersion, obtaining more adequate results with PEG.

Taking the previously mentioned data into consideration, it can be said that the PVA has given the best dispersion and particle sizes. The main objective was to examine the effects different polymers made in the catalysts prepared for the Sabatier reaction and looking to the results obtained we can say that the PVA is the most versatile polymer to improve the mentioned reaction.

5. CONCLUSION

The principal objective of this work is to examine the effects different polymers, with variation on their molecular weights and hydrolysis degree can produce on catalysts to improve the Sabatier reaction. For that, three polymers were used: PVA, PVP and PEG and every catalyst was analysed with characterization techniques.

The main conclusions of this work are:

- The addition of PVP and PEG into the formulation of catalysts prepared with the method "All in one" helps to control the particle size of the nickel, as well as PVA, which was analysed in previous works on our laboratory group.

- The increasing of the molecular weight of the added polymer in almost every catalyst produced an improvement for the Sabatier reaction, due to the dispersion was increased and the particle size, in contrast, decreased. Nonetheless, when increasing the molecular weight of the PVP, the differences obtained were almost unnoticeable, getting worst performances from the catalysts with this last polymer.

- Comparing the polymers used, the PVA allows to control the particle size of the nickel better than PVP or PEG. Furthermore, the increasing of the molecular weight in PVA has given smaller particle sizes, obtaining a larger dispersion and consequently, obtaining larger metallic surface per catalyst gram.

6. BIBLIOGRAPHY

[1]National ocean service. "What is the carbon cycle" https://oceanservice.noaa.gov/facts/carbon-cycle.html#:~:text=The%20carbon%20cycle%20describes%20the,this%20system%20does%20not%20change. Last time viewed:17/06/2021

[2]amp, clean energy. "Biomass – a low carbon energy source https://www.ampcleanenergy.com/our-sustainability-commitment. Last time viewed:17/06/2021

[3]Biomass_feasibility. http://www.esru.strath.ac.uk/EandE/Web_sites/0708/Biomass_feasibility/overview/carbon.html. Last time viewed:17/06/2021

[4]RUB, RUHR UNIVERSITÄT BOCHUM. "Closed carbon cycle economy (CCCE)" https://forschung.ruhr-uni-bochum.de/en/closed-carbon-cycle-economy-ccce. Last time viewed:17/06/2021

[5] The Economic Times. "Definition of natural Gas" https://economictimes.indiatimes.com/definition/natural-gas. Last time viewed:17/06/2021

[6] N. Sánchez Guerra, Estructuración de catalizadores Ni/La-Al_2O_3 para la producción de biogás natural sintético. TFG (2017) San Sebastian, UPV/EHU.

[7]Enagas. "Mapa de infraestructuras de gas natural en España"

https://www.enagas.es/enagas/en/Transporte_de_gas/TransporteYOperacion/MapaInfraestructuras. Last time viewed:17/06/2021

[8] J. Kjarstad, F. Johnsson, Energy Policy 35 (2007) 869.

[9]B. Teislev, 2002. Wood-chips gasifier combined heat and power. VDI Berichte 2. https://www.researchgate.net/publication/30482362_Wood-chips_gasifier_combined_heat_and_power Last time viewed: 28/06/2021

[10] International Energy Agency, Energy Technology Perspectives, Paris, France, 2012. https://www.iea.org/reports/energy-technology-perspectives-2012 Last time viewed: 28/06/2021

[11]Maps of World "Electricity Generation from Natural Gas by Country" https://www.mapsofworld.com/headlinesworld/technology/electricity-generation-natural-gas-country/ Last time viewed: 17/06/2021

[12]C.M. van der Meijden. ECN. Development of the MILENA gasification technology for the production of Bio-SNG. PhD Thesis (2010) Eindhoven, TU/e.

[13] C. Van Der Meijden, L. Rabou, B. Van Der Drift, B. Vreugdenhil, R. Smith, Proceedings of the International Gas Union Research Conference 2 (2011) 880 .

[14] B. Steubing, R. Zah, C.Ludwig, Biomass Bioenergy 35 (2011) 2950.

[15] G. A. Olah, G. K. S. Prakash, A. Goeppert, J. Am. Chem. Soc. 133 (2011) 12881.

[16] Deutsches Zentrum für Luft-und Raumfahrt. DLR-Power to gas in transport-Status quo and perspectives for development. (2014). https://www.bmvi.de/SharedDocs/EN/Documents/MKS/mks-studie-ptg-transport-status-quo-and-perspectives-for-development.pdf?__blob=publicationFile Last time viewed: 28/06/2021.

[17]POWER. News & Technology for the Global Energy Industry. "Progress for Germany´s Power-to-gas Drive" https://www.powermag.com/progress-for-germanys-power-to-gas-drive/ . Last time viewed: 17/06/2021

[18]L. Martín Burillo. "La reacción de metanación" (2010). https://zaguan.unizar.es/record/5496/files/TAZ-PFC-2010-429.pdf. Last time viewed: 17/06/2021

[19]G. Leonzio. Chem. Eng. J. 290 (2016) 490.

[20]Y. Huang, Q.P. Zheng, N. Fan, K. Aminian. Appl. Energy 113 (2014) 1475.

[21]M. Pekala, R.R: Tan, D. C. Y. Foo, J.M. Jezowski. Appl. Energy 89 (2010) 1903.

[22]J. K.Kesavan, I. Luisetto, S.Tuti, C. Meneghini, G. Lucci, C.Battocchio, S. Mobilio, S. Casciardi, R. Sisto. J. CO_2 util. 23 (2018) 200.

[23] M. Heitbaum, F. Glorius, I. Escher. Angew. Chem. Int. Ed. 45 (2006) 4732.

[24]A. Roucoux, J. Schulz, H. Patin. Chem. Rev. 102 (2002) 3757.

[25] C. Louis. Catalysts 6 (2016) 110.

[26] E. Gonzalez, A. Barquero, B. Muñoz-Sanchez, M. Paulis, J. R. Leiza. Nanomaterials 11 (2021) 706.

[27] A. Egaña, Síntesis de Fischer-Tropsch con gas de síntesis provenientes de biomasa. PhD Thesis (2018) San Sebastian, UPV/EHU.

[28]L. Huang, H. Wang, J. Chen, Z. Wang, J. Sun, D. Zhao, Y. Yan, Micropor. Mesopor. Mat. 58 (2003) 105.

[29] Z. Liang, C. Qu, D. Xia, R. Zou, Q. Xu, Angew. Chem. Int. Ed. 57 (2008) 9604.

[30] K. Pate, P. Safier. Advances in Chemical Mechanical Planarization (CMP) Chapter 12 (2016) 299.

[31] University of Illinois. "Diffraction of light, light bending around an object" http://ww2010.atmos.uiuc.edu/(Gh)/guides/mtr/opt/mch/diff.rxml. Last time viewed 18/06/2021.

[32] N. Stock, S. Biswas, Chem. Rev. 112 (2012) 933.

[33] S. Bauer, C. Serre, T. Devic, P. Horcajada, J. Marrot, G. Ferey, N. Stock, Inorg. Chem. 47 (2008) 7568.

[34] Wyatt technology. "SEC-MALS, Absolute molar mass and size" https://www.wyatt.com/solutions/techniques/sec-mals-molar-mass-size-multi-angle-light-scattering.html. Last time viewed 18/06/2021.

[35]J. Zataray, A. Agirre, P. Carretero, L. Meabe, J. C. de la Cal, J. R. Leiza. J. appl. polym. sci. DOI: 10.1002/APP.4243442434 (2015) 42434.

[36] E. Folta-Stogniew, Yale University. BioProcess International™ Analytical and Quality Summit. "Protein Characterisation by Static Light Scattering" https://medicine.yale.edu/keck/biophysics/talks/BioProcessInternational_2008_131169_284_4182_v2.pdf Last time viewed 18/06/2021.

[37] K. Oura, V.G. Lifshits, A. Saranin, A.V. Zotov, M. Katayama. Surface Science, An Introduction, Berlin: Springer (2003)

[38] M. C. Desjonqueres, D. Spanjaard (1996), Concepts in surface physics (2nd ed.), New York: Springer-Verlag 29 (2012).

[39] G. Yu, B. Sun, Y.Pei, S. Xie, S. Yan, M. Qiao, K. Fan, S. Zhang, B. Zong, J. Am. Chem. Soc.132 (2010) 935.

[40] Micromeritics Instrument Corporation. "Chemisorption" https://www.micromeritics.com/Repository/Files/Chemisorption_Poster.pdf. Last time viewed 14/06/2021.

[41] Particle Technology Labs. "Chemisorption" https://www.particletechlabs.com/analytical-testing/chemisorption. Last time viewed 18/06/2021. Last time viewed 14/06/2021.

[42] A. Brückner, J.-F. Carpentier, A.M. Efstathiou, G.J. Hutchings, J.A. Lercher, J.C.S. Wu, Y.J. Xu, Catal. Commun. 97(2017) 10.

[43] Micromeritics Instrument Corporation. "Temperature-Programmed Reduction Using the AutoChem" https://www.micromeritics.com/Repository/Files/appnote120.pdf . Last time viewed 18/06/2021.

[44] X-ray Diffraction. http://web.pdx.edu/~pmoeck/phy381/Topic5a-XRD.pdf. Last time viewed 18/06/2021.

[45] Geochemical Instrumentation and Analysis. "X-ray reflection in accordance with Bragg's Law"

https://serc.carleton.edu/research_education/geochemsheets/BraggsLaw.html. Last time viewed 18/06/2021. Last time viewed 14/06/2021.

[46]A.Zhao, W. Ying,H. Zang, H. Ma, D. Fang, Catal. Commun. 17 (2012) 34

[47]C. Agrafiotis, A. Tsetsekou, J. European Ceramic Soc. 20 (2000) 815

[48] P. Ávila, M. Montes, E.E. Miró, Chem. Eng. J. 109 (2005) 11

[49] Guozhao Ji and Ming Zhao (March 8th 2017). Membrane Separation Technology in Carbon Capture, Recent Advances in Carbon Capture and Storage, Yongseung Yun, IntechOpen, DOI: 10.5772/65723. Available from: https://www.intechopen.com/books/recent-advances-in-carbon-capture-and-storage/membrane-separation-technology-in-carbon-capture

[50] T.A. Nijhuis, A.E.W. Beers, T. Vergunst, I. Hoek, F. Kapteijn, J.A. Moulijn, Catal. Reviews – Sci. Eng. 43 (2001) 345.

[51] Polymer Properties Database. "Reptation and tube model"

https://polymerdatabase.com/polymer%20physics/Reptation.html. Last time viewed 18/06/2021.

[52] Wikipedia, The Free Encyclopaedia. "Reptation" https://en.wikipedia.org/wiki/Reptation. Last time viewed 18/06/2021.

[53] N.R. Peela, A. Mubayi, D.Kunzru, Catal. Today 147 (2009) S17.

[54]V.G. Milt, S. Ivanova, O. Sanz, M.I. Domínguez, A. Corrales, J.A. Odriozola, M.A. Centeno, Appl. Surf. Sci. 270 (2013)169.

[55]M. Signoretto, F. Menegazzo, A. Di Michele, E. Fioriniello. Catalysts 6 (2016) 87.